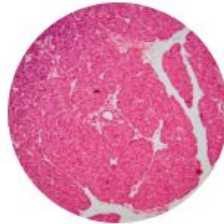




CIFAR



5PM

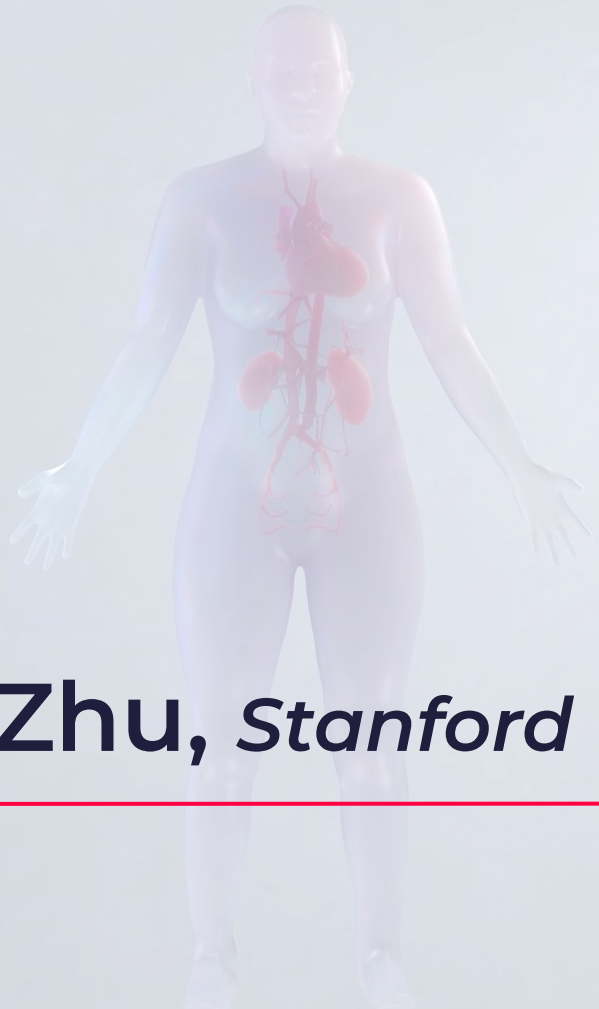
10PM in London (GMT), 7AM in Tokyo (GMT+9)

Cells & Vasculature

Moderator: Katy Börner, *Indiana University*

Presenters:

- Chenchen Zhu, *Stanford University*
- Samuel L. Ewing, *University of Florida*
- Kevin Matthew Byrd, *Adams School of Dentistry Oral and Craniofacial Health Sciences*
- Archibald Enninful, *Yale University*
- Alex Wong, *Harvard University*
- Ravi Misra, *University of Rochester*



Chenchen Zhu, Stanford University



Understanding human intestine using single-cell spatial transcriptomics

Chenchen Zhu

Research Scientist @ Michael Snyder Lab, Stanford University

Stanford Tissue Mapping Center for HuBMAP



Emma Monte



Bei Wei



Bingqing Zhao



Joanna Bi



HuBMAP

Human BioMolecular Atlas Program

Map the complexity of the small bowel and colon

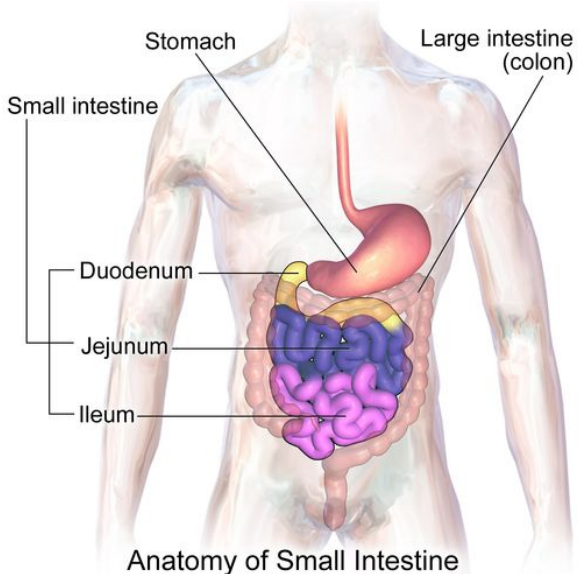
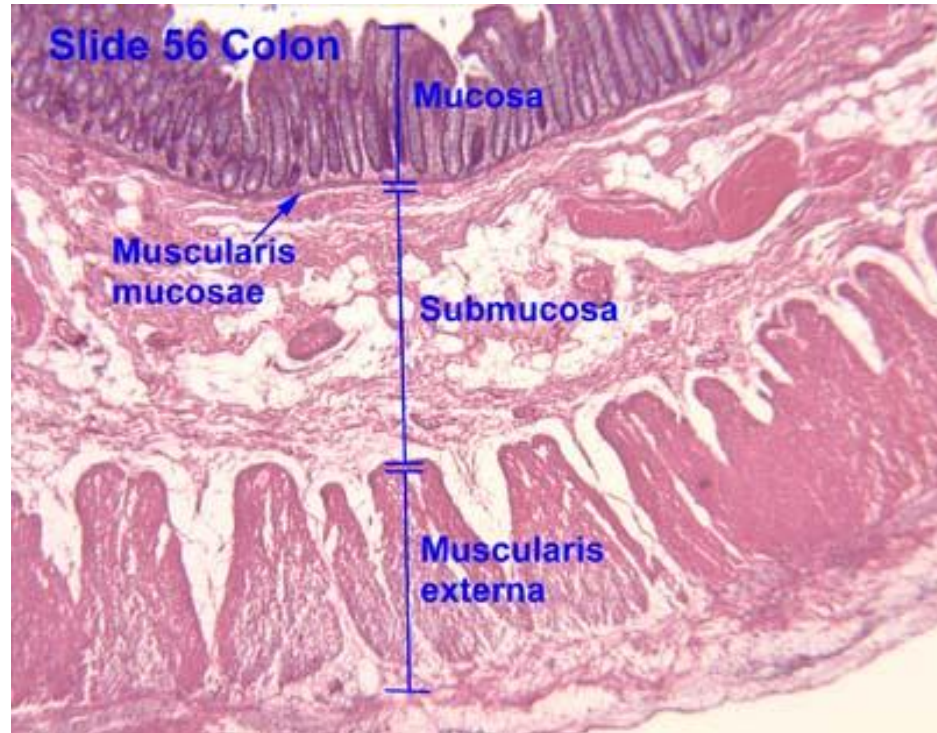


Table A.1. Stanford TMC production

small bowel sites	36
colon sites	36
sn RNA-seq	122
sn ATAC-seq	122
CODEX 2D and 3D maps	122
Spatial RNA maps	110
bulk RNA-seq	8
bulk ATAC-seq	16
WGS	17
metabolomics	56
lipidomics	32
proteomics	26

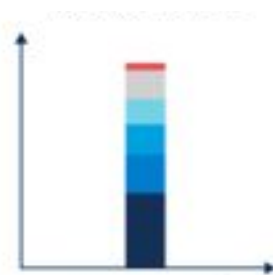
Histology of full thickness sections of human duodenum



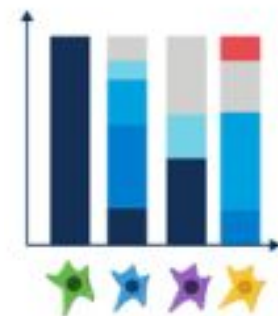
<https://www.ouhsc.edu/histology/Text%20Sections/Lower%20GI.html>

Spatial technology to better understand tissue biology

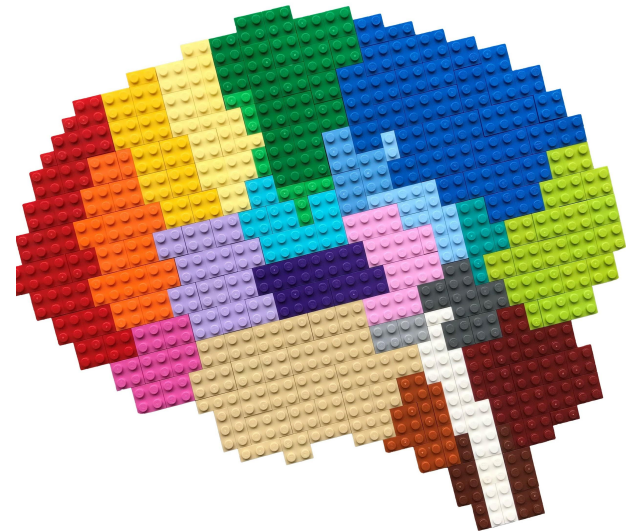
Bulk assays



Single-cell RNA-seq



Spatial omics

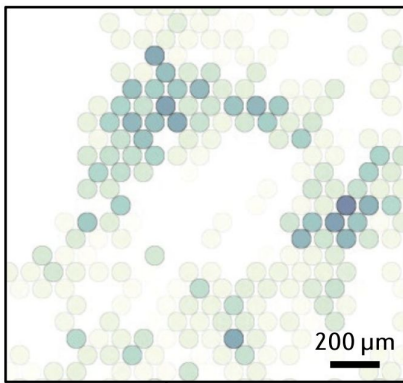


Why spatial transcriptomics (RNA)?

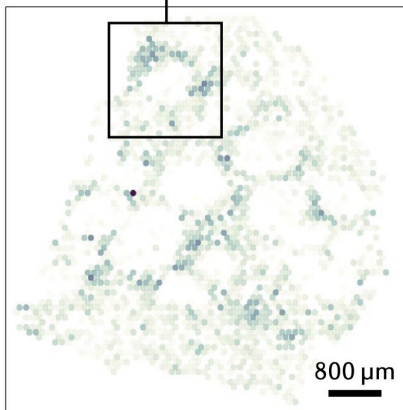
- High target number - higher resolution for mapping cell types and states
- Flexibility in target choice - not limited to antibody availability
- Gene regulation
- Multiomics integration

Two quantification principles of spatial transcriptomics

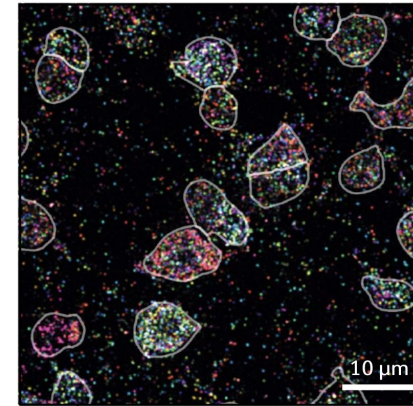
Detection by sequencing



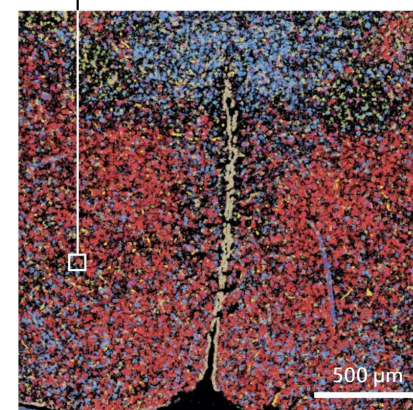
Unbiased survey
Low mRNA capture rate
Limited spatial resolution



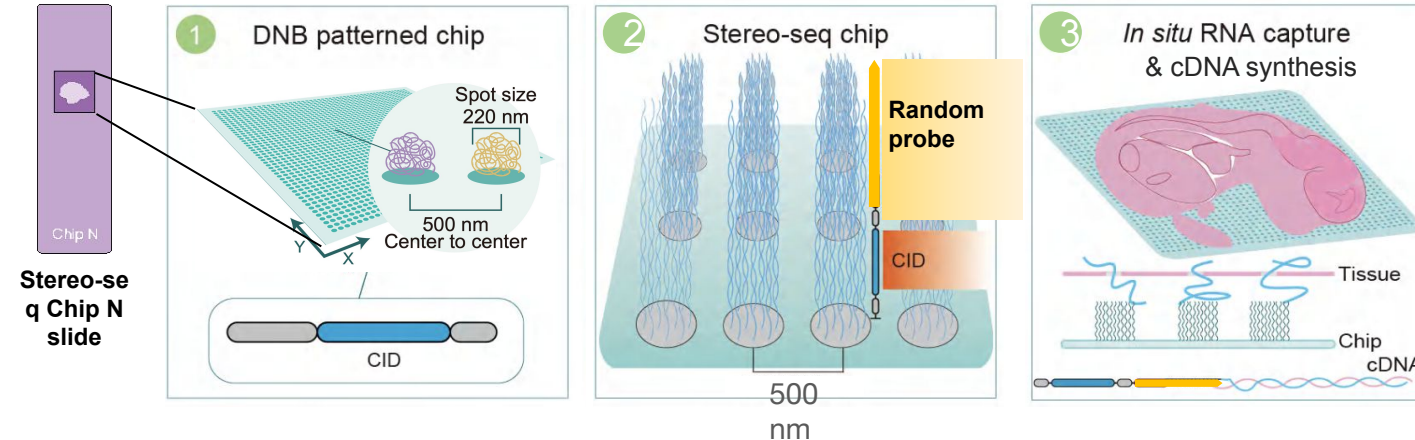
Detection by imaging (targeted multiplexed FISH)



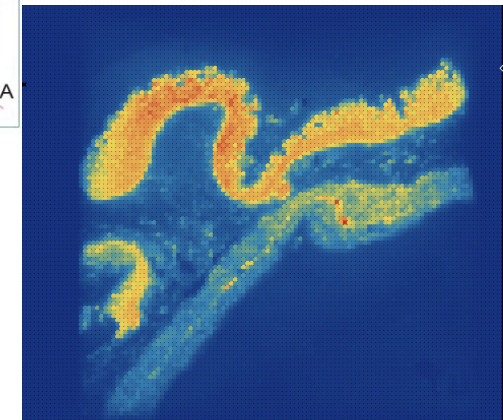
Targeted approach
High spatial resolution
High capture rate
Limited field of view



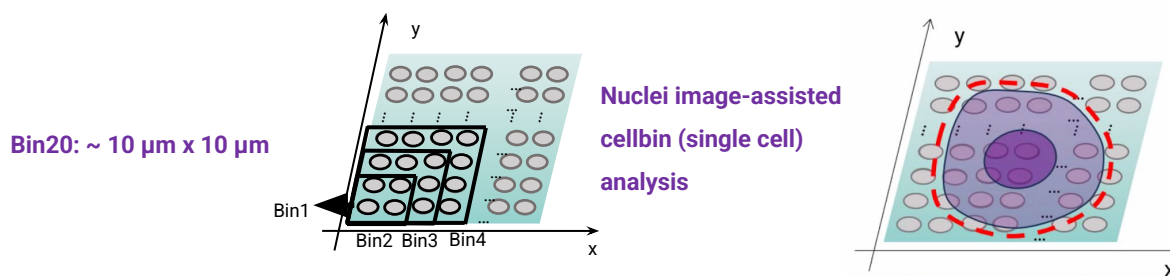
Stereo-seq for FFPE tissue sections



Stereo-seq
signal heatmap
for duodenum

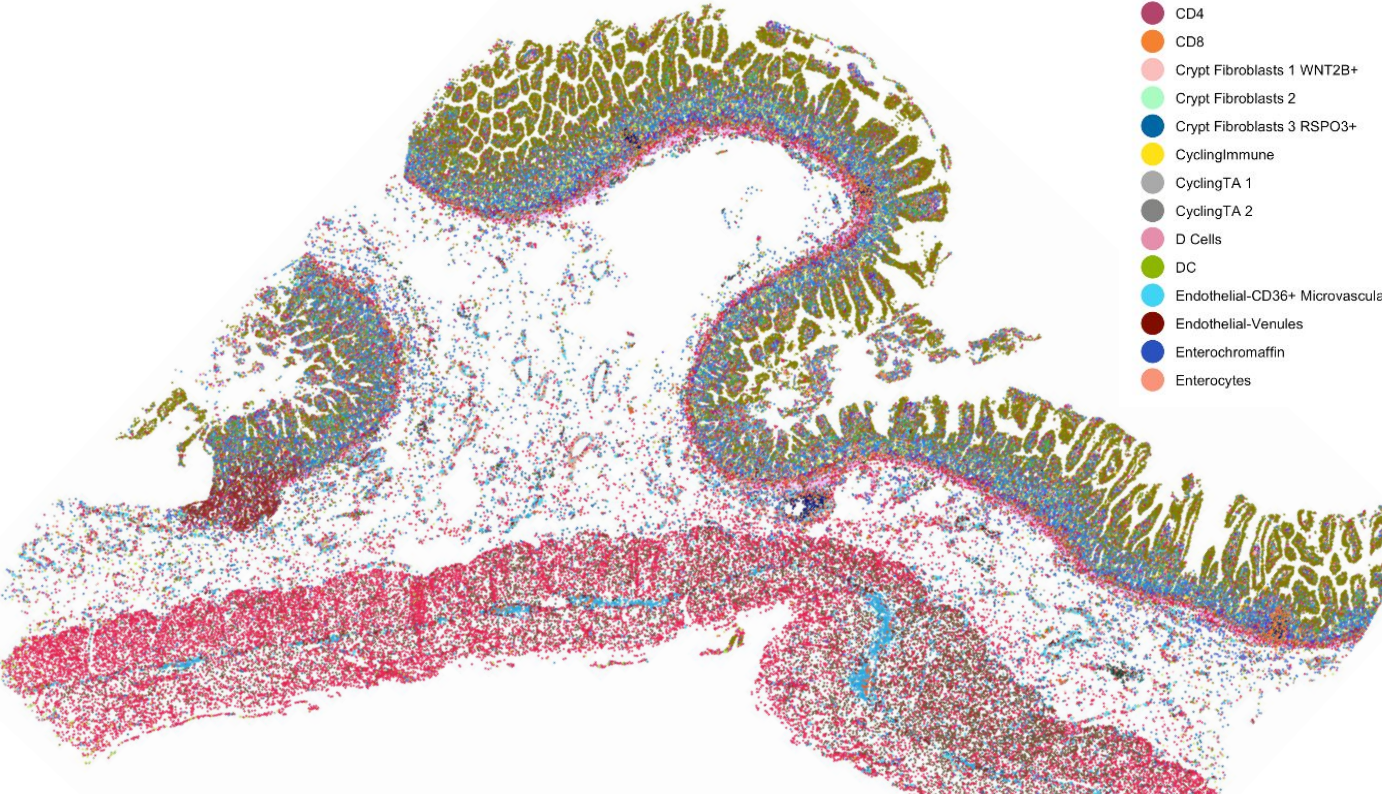


STOmics



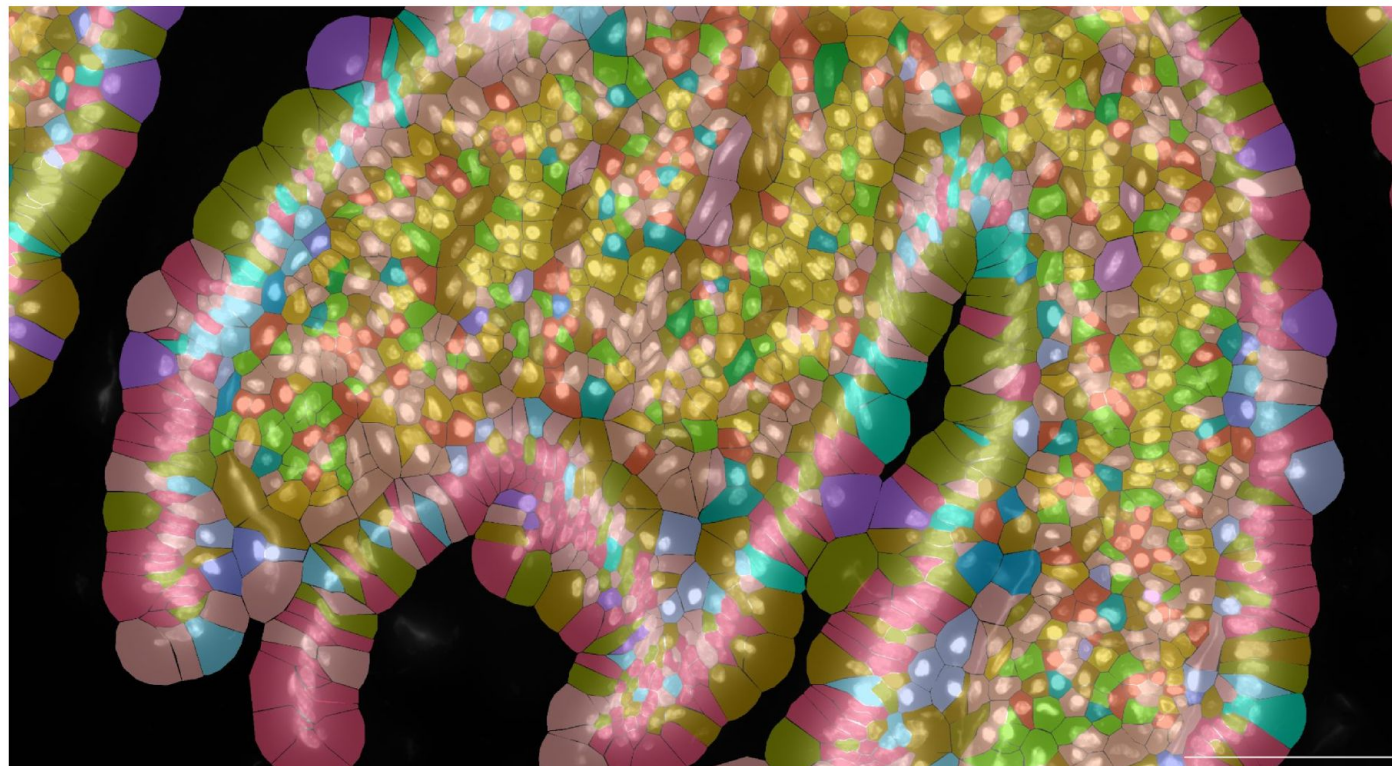
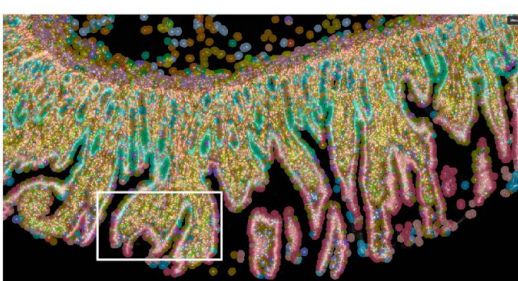
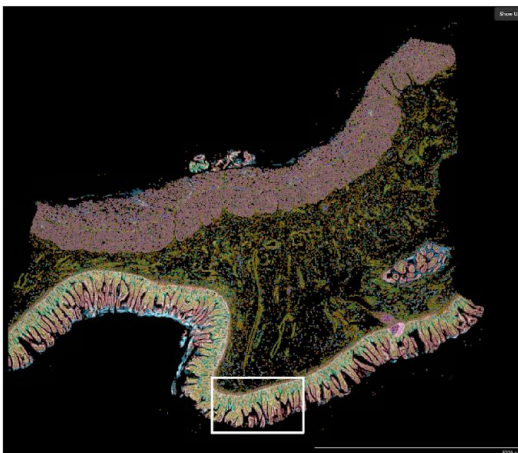
Stereo-seq maps cell types of human intestine duodenum

- 1*1 cm chip with 4.6B reads for 186,000 cells
- Profiled > 32,000 genes with 56.6M transcripts



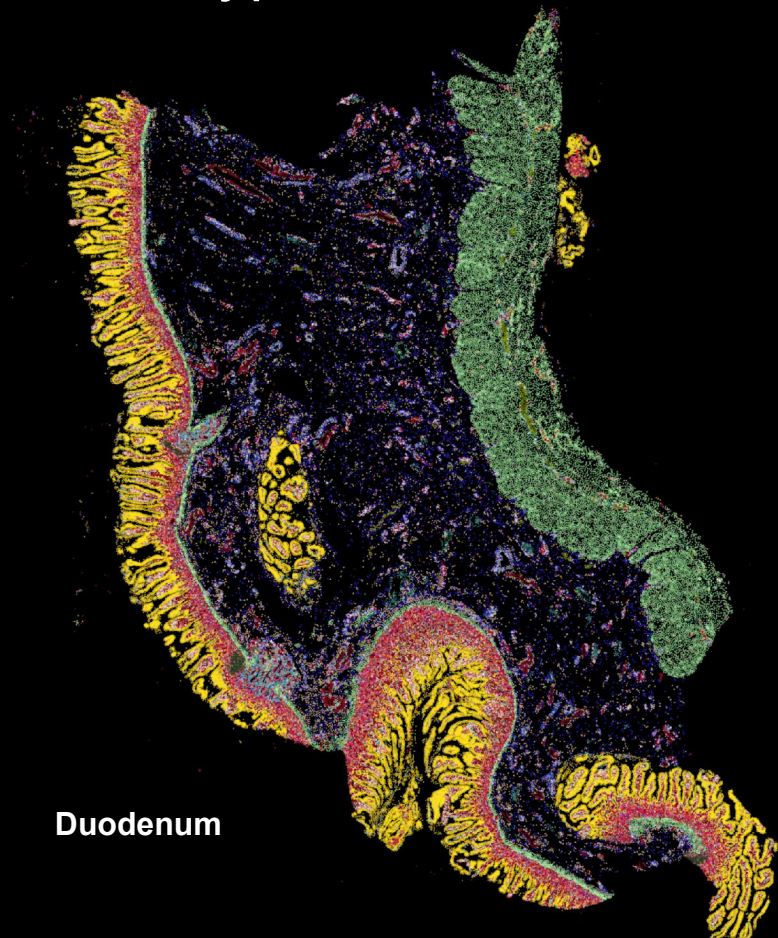
Adipocytes	EnteroendocrineUn	Myofibroblasts/SM 3
B Cells	EnteroendocrineUn 1	Myofibroblasts/SM DES High
Best4+ Enterocytes	Epithelial	NEUROG3high
CD4	Glia	Neurons
CD8	Goblet	Paneth
Crypt Fibroblasts 1 WNT2B+	I Cells	Pericytes
Crypt Fibroblasts 2	ICC	Plasma
Crypt Fibroblasts 3 RSPO3+	ILC	S Cells
CyclingImmune	Immature Enterocytes	Secretory Specialized MUC5B+
CyclingTA 1	Immature Goblet	Secretory Specialized MUC6+
CyclingTA 2	K Cells	Stem
D Cells	Lymphatic Endothelial Cells	TA1
DC	Mast	TA2
Endothelial-CD36+ Microvascular	Mo Cells	Tuft
Endothelial-Venules	Mono_Macrophages	Unknown
Enterochromaffin	Myofibroblasts/SM 1	Villus Fibroblasts WNT5B+
Enterocytes	Myofibroblasts/SM 2	

Human intestine FFPE profiled using Xenium



Duodenum of B015

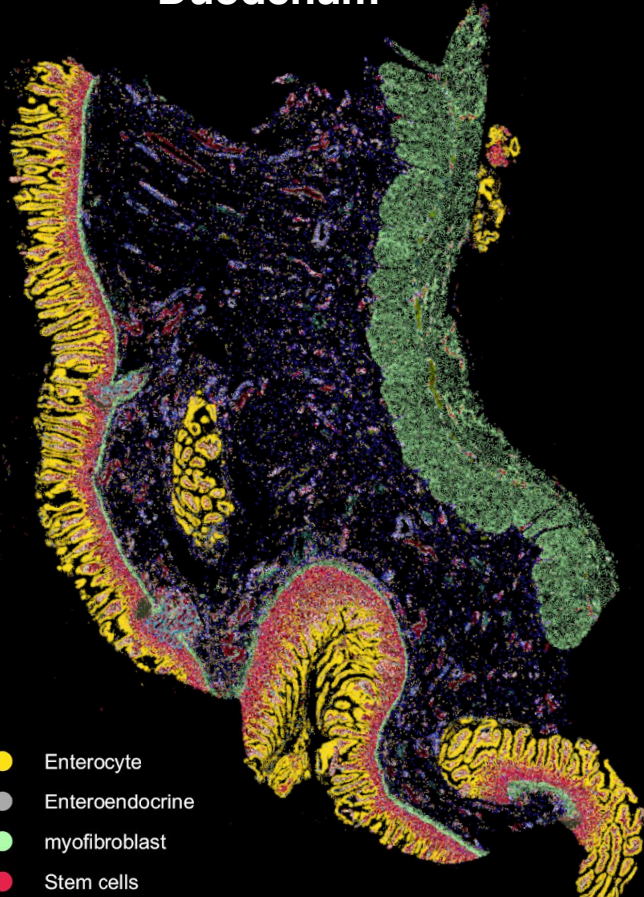
Cell types in human intestine revealed using Xenium



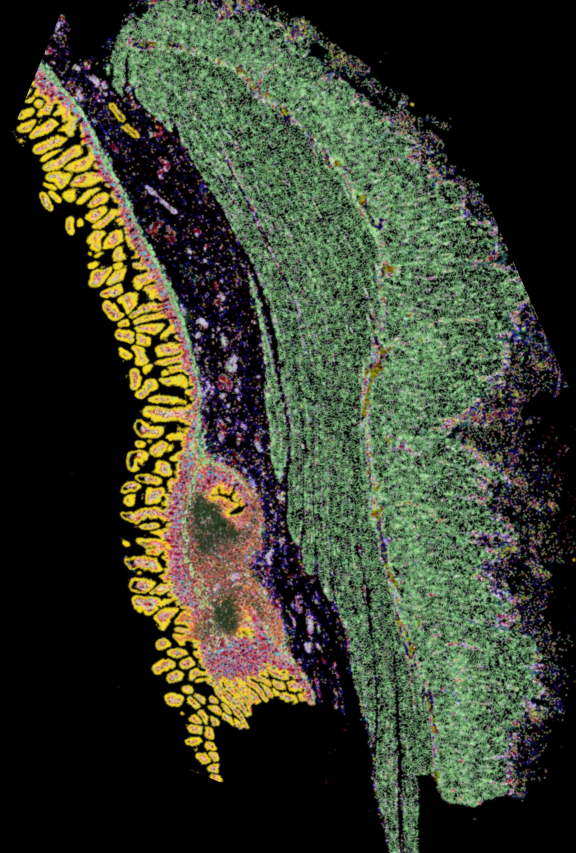
- Arterial EC
- Branch
- Capillary
- CD4 T
- CD8 T
- Cycling B
- DC
- ENCC/glia
- Enterocyte
- Enteroendocrine
- Epithelial
- FDC
- Glia
- Goblet cell
- IgA plasma cell
- IgM plasma cell
- ILC
- LEC
- Macrophages
- Mast
- Megakaryocyte
- Memory B
- Mesoderm 1
- Mesoderm 2
- Mesothelium
- Microfold cell
- Monocytes
- myofibroblast
- Naive B
- NK
- Paneth
- Pericyte
- Progenitor B
- Proximal progenitor
- SMC
- Stem cells
- Stromal 1
- Stromal 2
- Stromal 3
- TA
- Treg
- Tuft
- Undifferentiated cells
- unident
- Venous EC

Cell types of human intestine revealed using Xenium

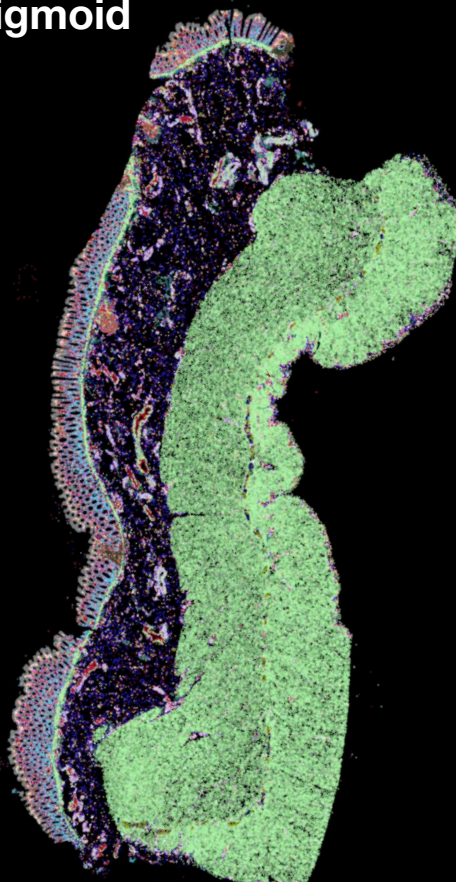
Duodenum



Ileum



Sigmoid



- Enterocyte
- Enteroendocrine
- myofibroblast
- Stem cells

Summary: Lead ST assays for Stanford HuBMAP TMC

- Stereo-seq for discovery, Xenium for data production
- Both FF-OCT and FFPE compatibility
- Whole tissue sections
- High reproducibility and sensitivity

Acknowledgement

CBVA | avp

Emma Monte
Bingqing Zhao
Bei Wei

John Hickey
Pauline Chu
Joanna Bi

Yiing Lin
Shin Lin
Laren Becker

Amir Bahmani
Lihua Jiang
Rongduo Han



HuBMAP

HTAN
HUMAN TUMOR ATLAS NETWORK



Stanford
MEDICINE

aws

The background of the slide features a complex, abstract visualization of a neural network or a similar complex system. It consists of numerous thin, translucent lines of various colors (blue, green, yellow, pink) forming a dense web against a light gray background. Interspersed among these lines are numerous small, glowing circular particles in shades of white, blue, and green, some with trails, suggesting movement and data flow.

Samuel L. Ewing, *University of Florida*

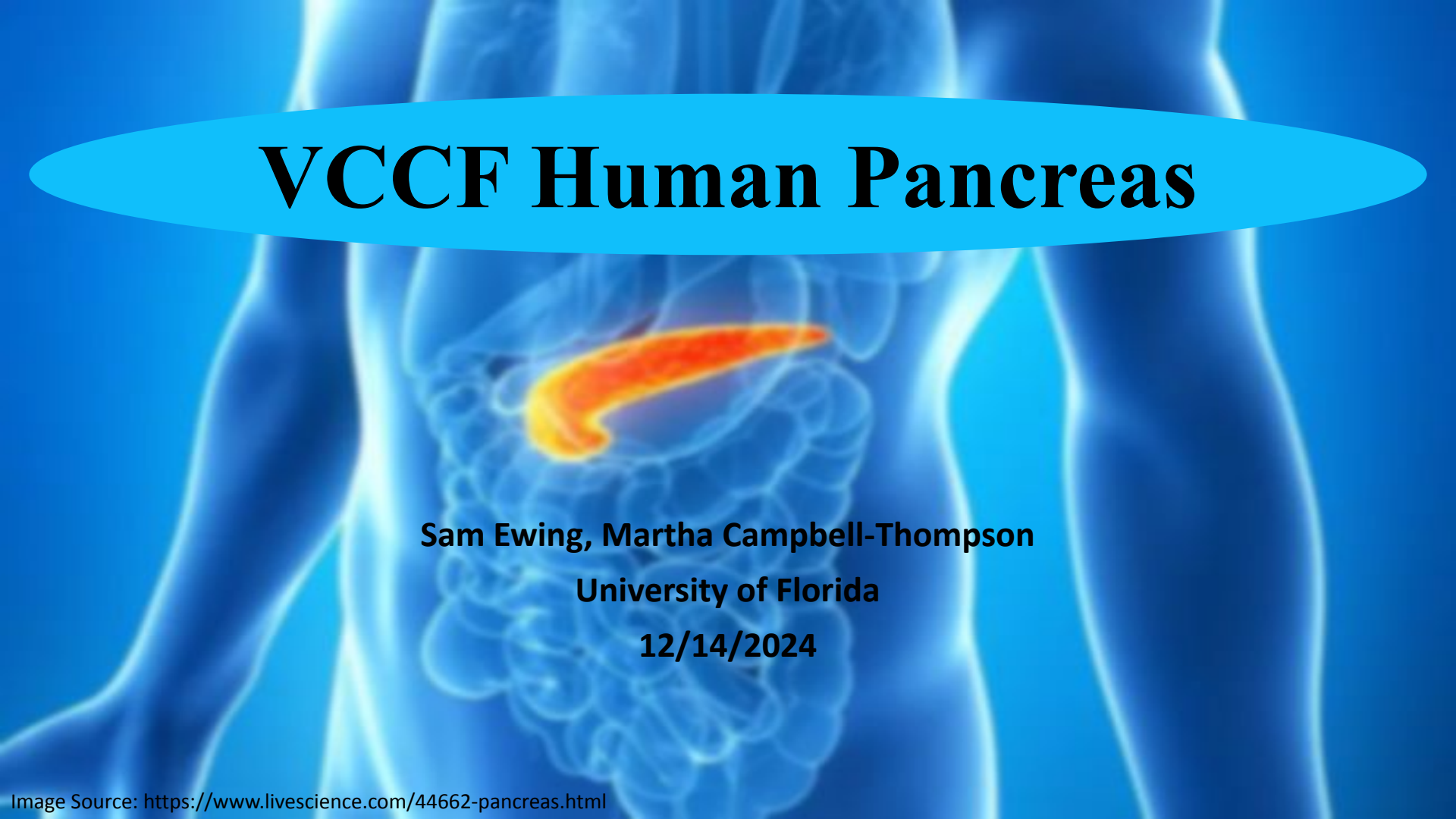


Multi-omics spatial mapping for human pancreas

Clayton Mathews, Martha Campbell-Thompson, James Carson, Ernesto Nakayasu, Ying Zhu, Sam Ewing, Jing Chen, Yumi Kwon, Dongtao Fu, Tyler Segendorf, Jeremy Clair, Wei-Jun Qian



VCCF Human Pancreas

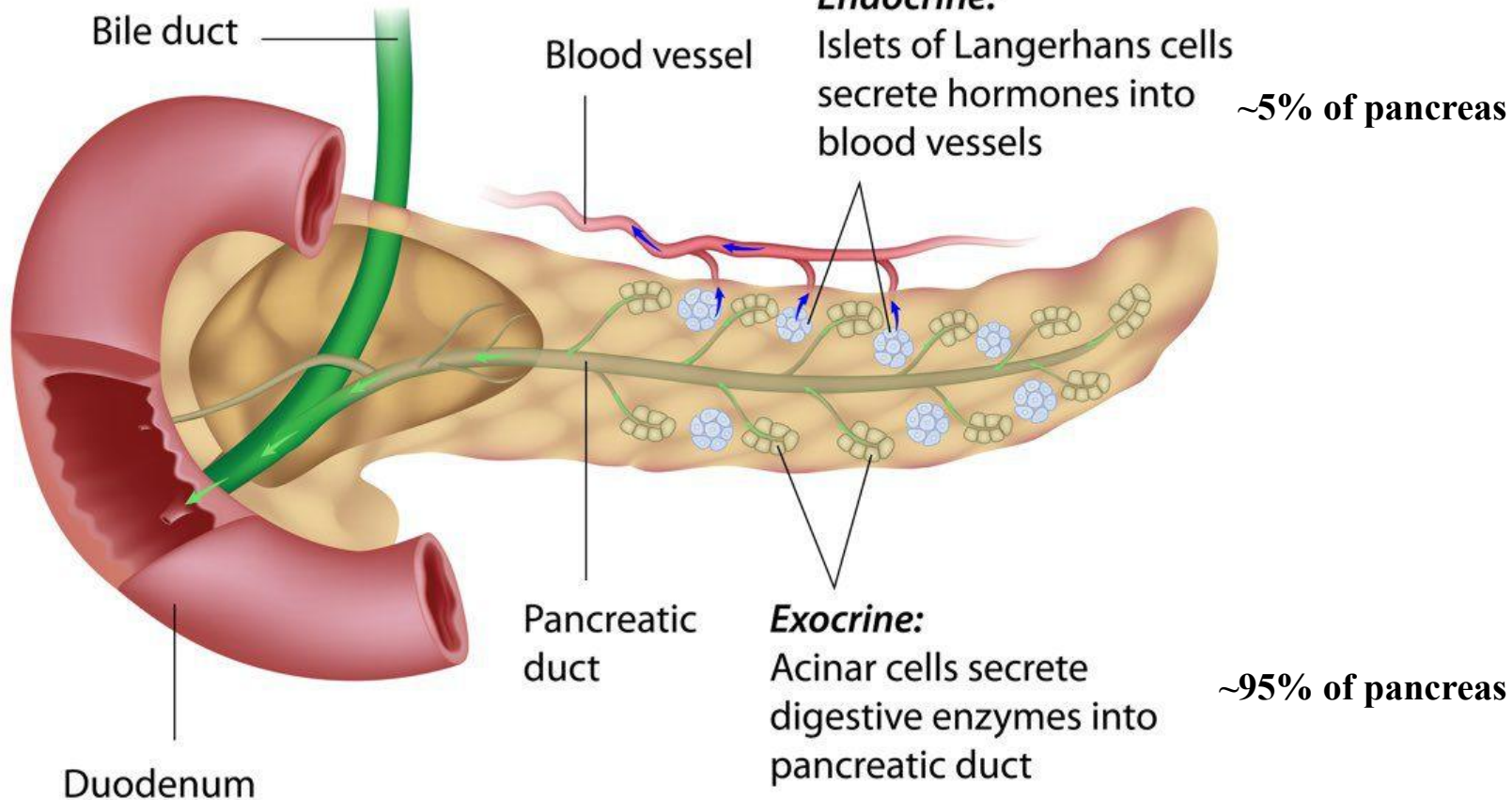


A blue-toned anatomical illustration of the human torso, showing the internal organs. The pancreas is highlighted with a vibrant red and orange color, appearing as a curved organ situated behind the stomach. The surrounding organs, including the liver, gallbladder, and intestines, are depicted in a lighter blue shade.

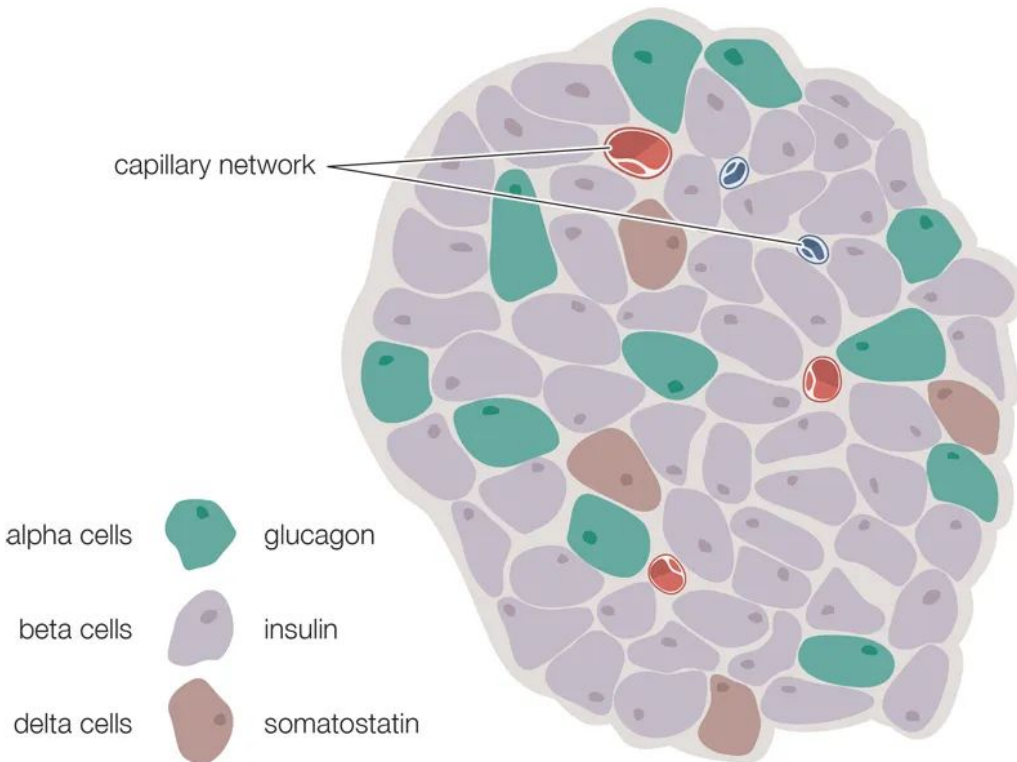
Sam Ewing, Martha Campbell-Thompson
University of Florida

12/14/2024

Introduction to the Human Pancreas



Islets of Langerhans and Type 1 Diabetes

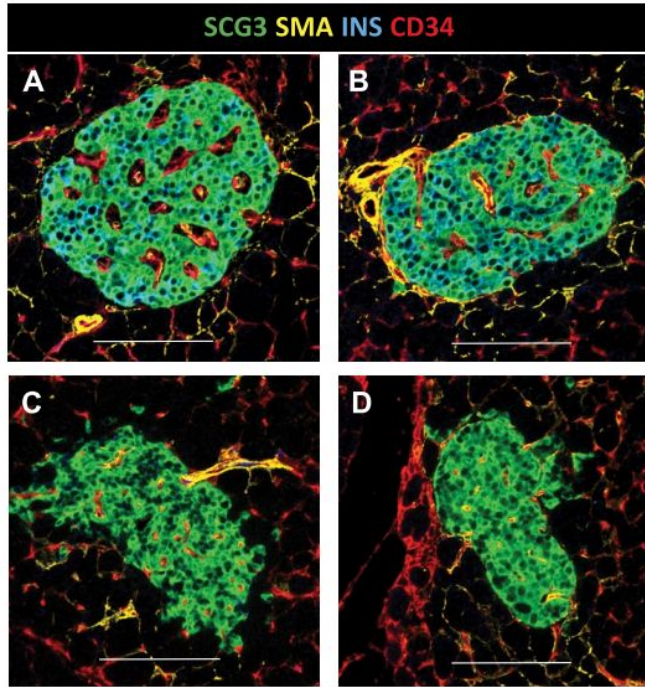


Type 1 Diabetes:

- ❖ Autoimmune disease
- ❖ Immune system attacks pancreatic islets, killing beta cells
- ❖ Beta cells responsible for insulin release and glucose metabolism
- ❖ T1D leads to glucose dysregulation

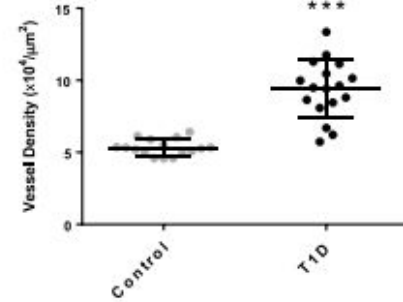
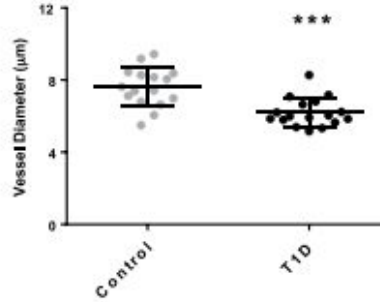
Microvascular Alterations in T1D

Control

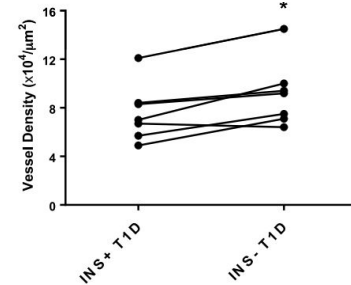
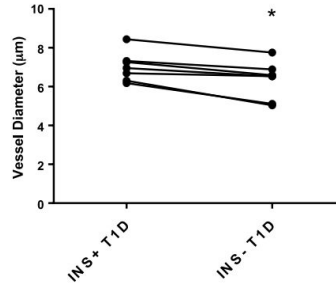


T1D

Vessel diameter decreases and vessel density increases in T1D

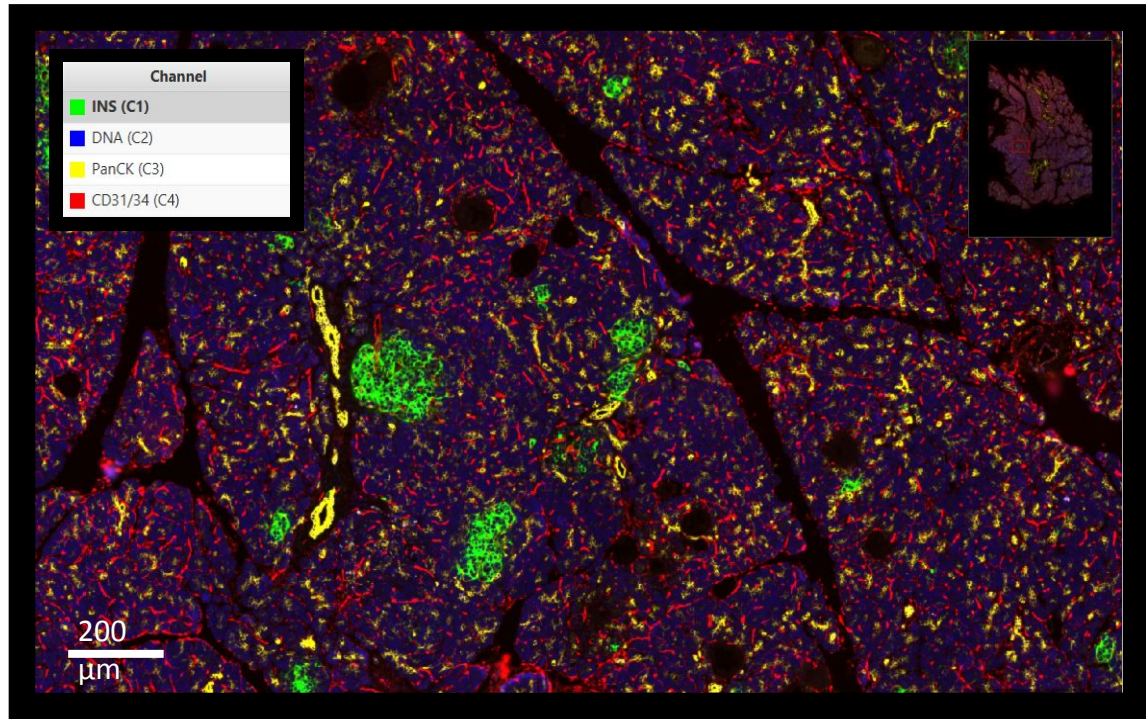


These alterations are most significant in INS- islets

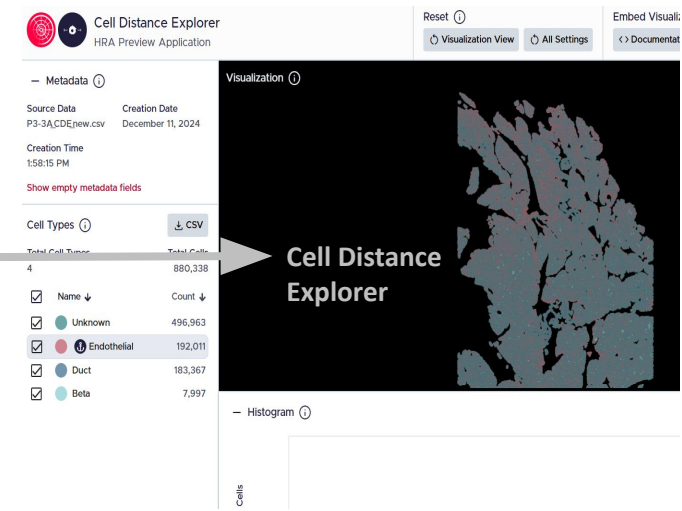
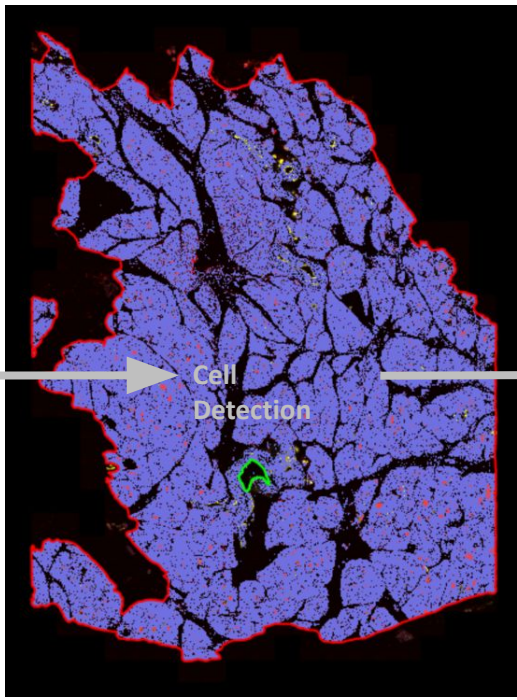
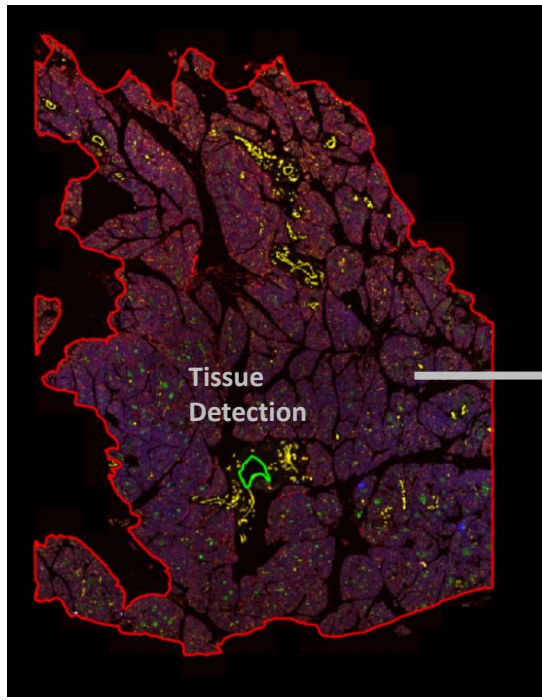


Data Collection

- ❖ Whole pancreases acquired from organ donors
- ❖ 8 control pancreases analyzed from HuBMAP
- ❖ 12 pancreases (6 control, 3 autoantibody positive, 3 type 1 diabetes) from another study analyzed
- ❖ Multiplex IF performed as part of spatial profiling using NanoString GeoMx technology
- ❖ Protein markers: insulin (INS), PanCK (duct), CD31/34 (vasculature)



Cell Segmentation with QuPATH Software



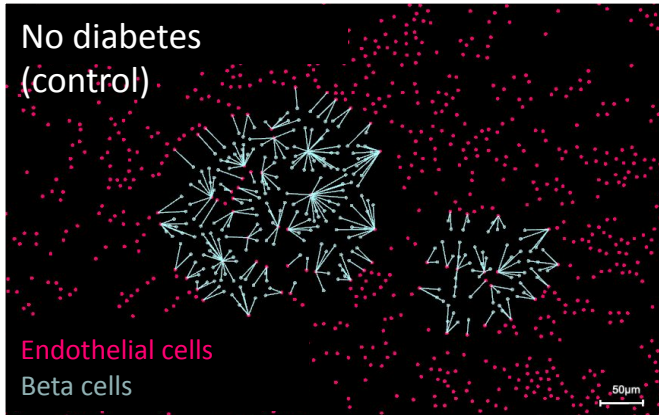


Human
Reference
Atlas

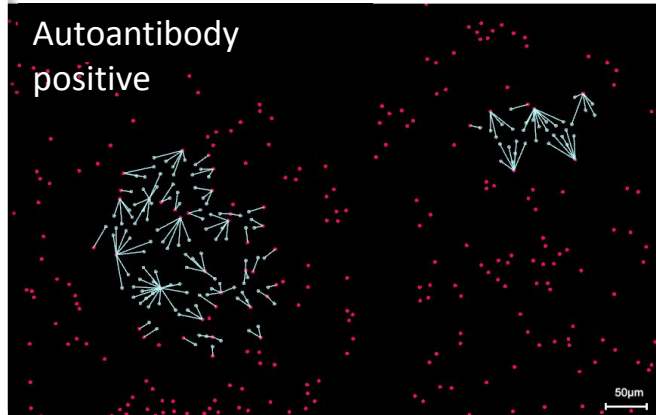


Cell Distance Explorer
HRA Preview Application

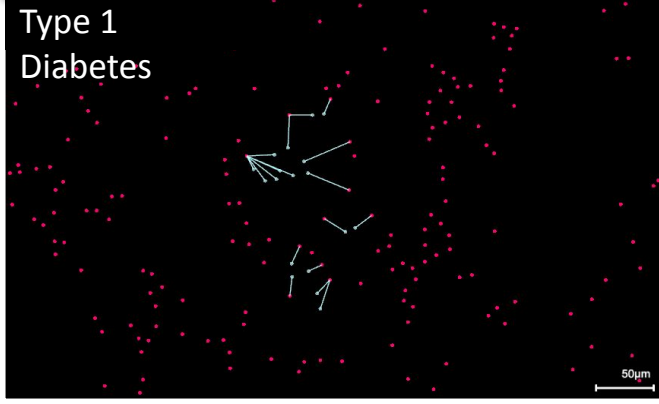
No diabetes
(control)



Autoantibody
positive

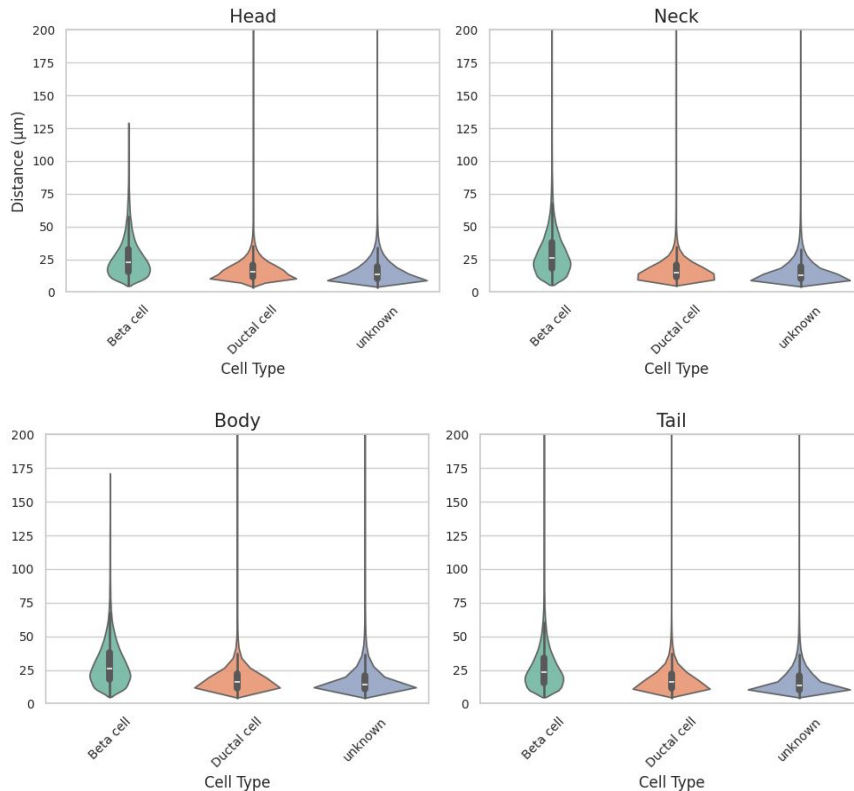


Type 1
Diabetes



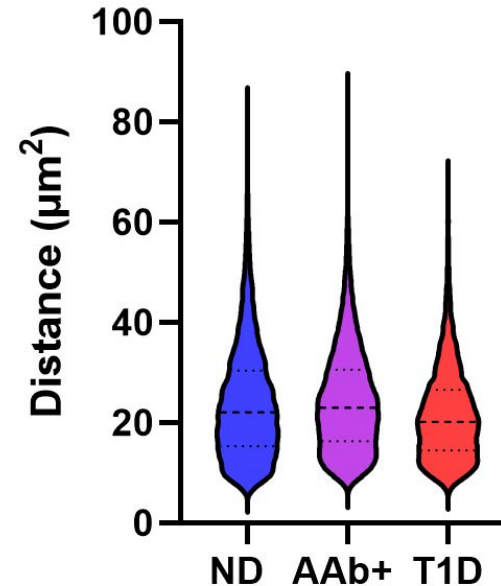
Beta Cell Distance Distributions

HuBMAP Control Pancreases



AAb+ and T1D Donors

Beta Cell Distances to Nearest Endothelial Cell





Thank you!

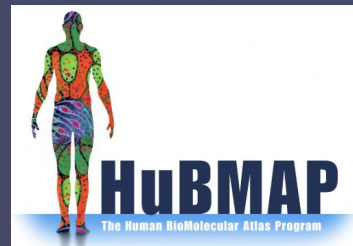
Dr. Martha
Campbell-Thompson

Dr. Dongtao Fu

Dr. Heather Kates

Dr. Katy Borner
Yashvardhan Jain

All other collaborators



**Kevin Matthew Byrd,
Virginia Commonwealth University**

Anchoring Oral and Craniofacial Cell Types within Digitized Vasculature Networks

Kevin Matthew Byrd, DDS, PhD

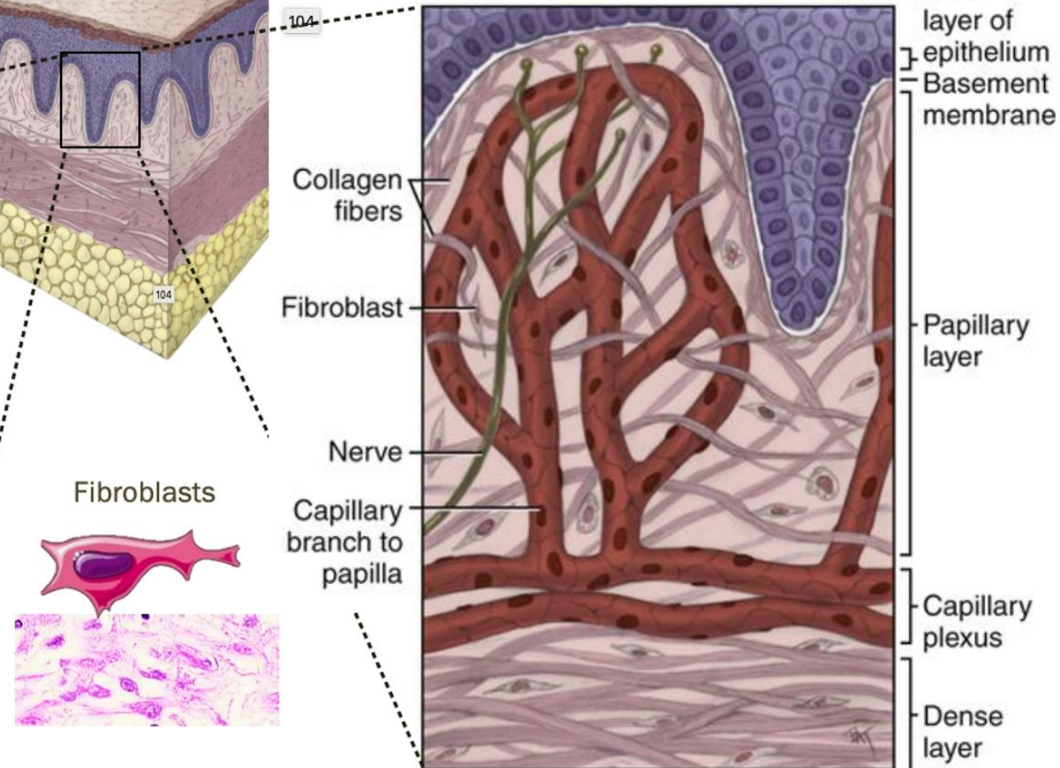
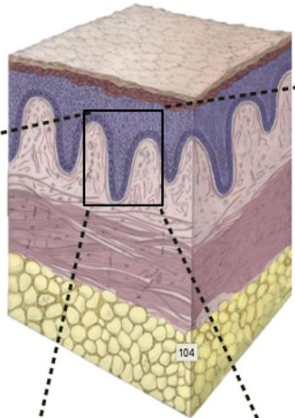
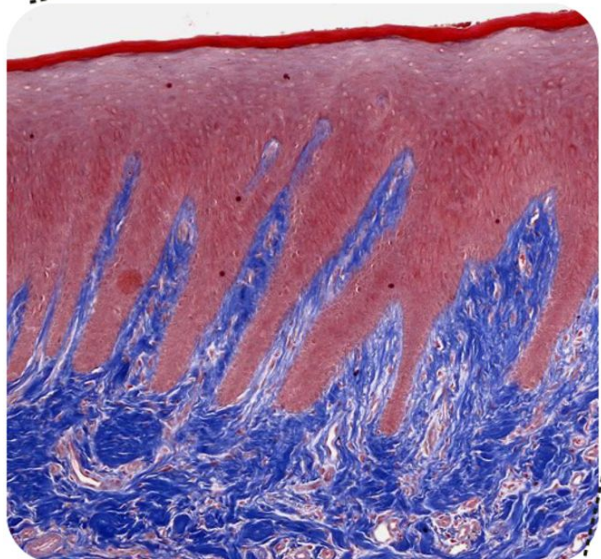
Assistant Professor, Virginia Commonwealth University

Member, VCU Massey Comprehensive Cancer Center; the NIH The HuBMAP Human BioMolecular Atlas Program
PI, Lab of Oral & Craniofacial Innovation (LOCI@VCU); Founder, Human Cell Atlas Oral & Craniofacial Bionetwork



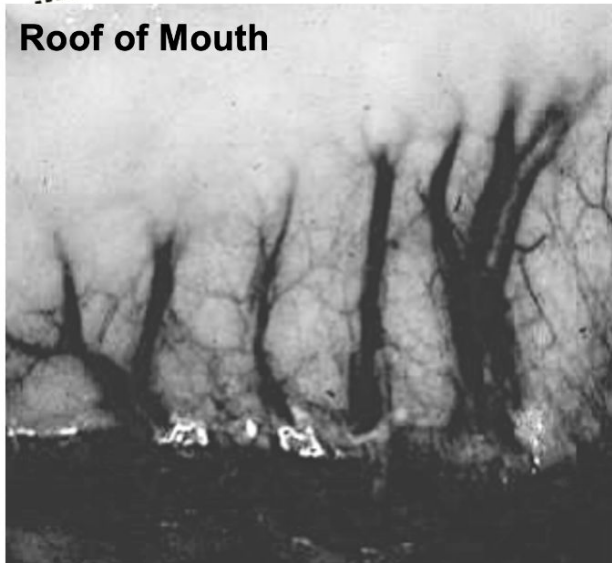
Heterogeneity of Oral and Craniofacial Tissues.

Fibroblasts – synthesize extracellular matrix
Endothelial cells of blood/lymphatic vessels
Peripheral nervous tissues

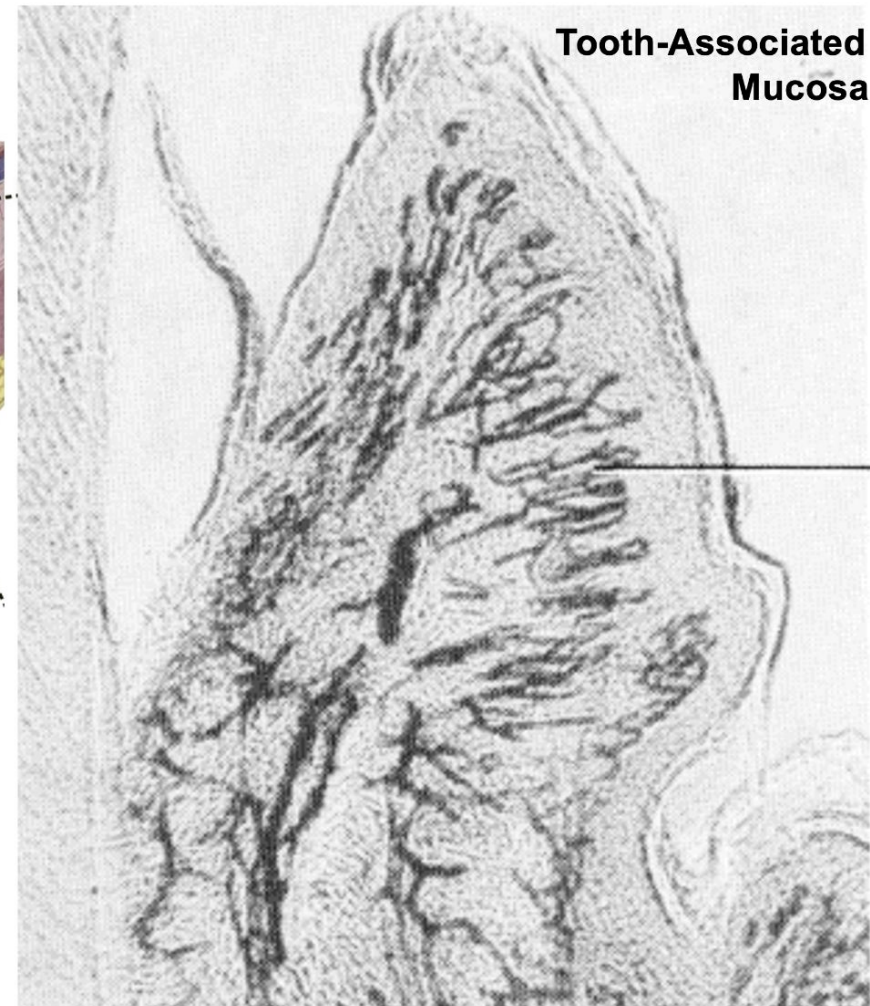
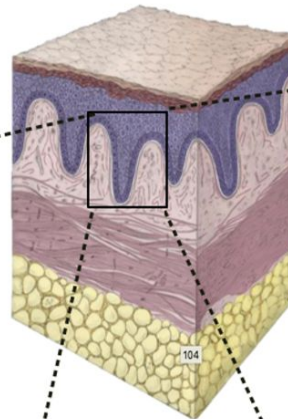


Heterogeneity of Oral and Craniofacial Tissues.

Fibroblasts – synthesize extracellular matrix
Endothelial cells of blood/lymphatic vessels
Peripheral nervous tissues



Roof of Mouth



**Tooth-Associated
Mucosa**

Oral is Aerodigestive; i.e., a part of Digestive and Respiratory Systems.

Orofacial Granulomatosis



Severe Gingivitis



Tongue Fissuring



Buccal Cobblestoning



Oropharyngeal Ulcerations



Angular & Exfoliative Chelitis



Mucogingivitis



Staghorn Lingual Ducts



Deep Linear Ulceration



Generalized Erythema



Erythema Multiforme



Gingival Hyperplasia



Lichenoid Mucositis



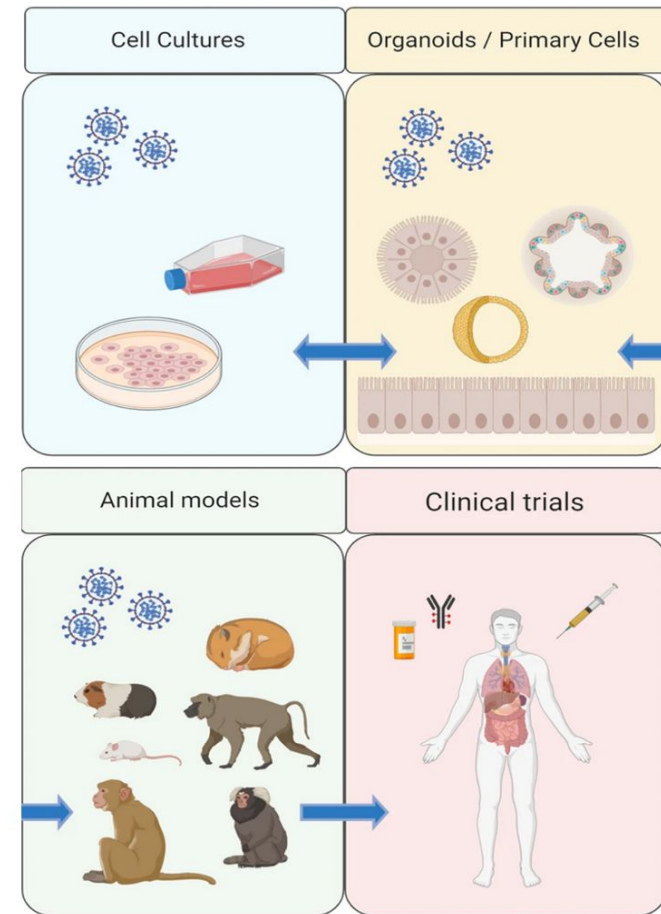
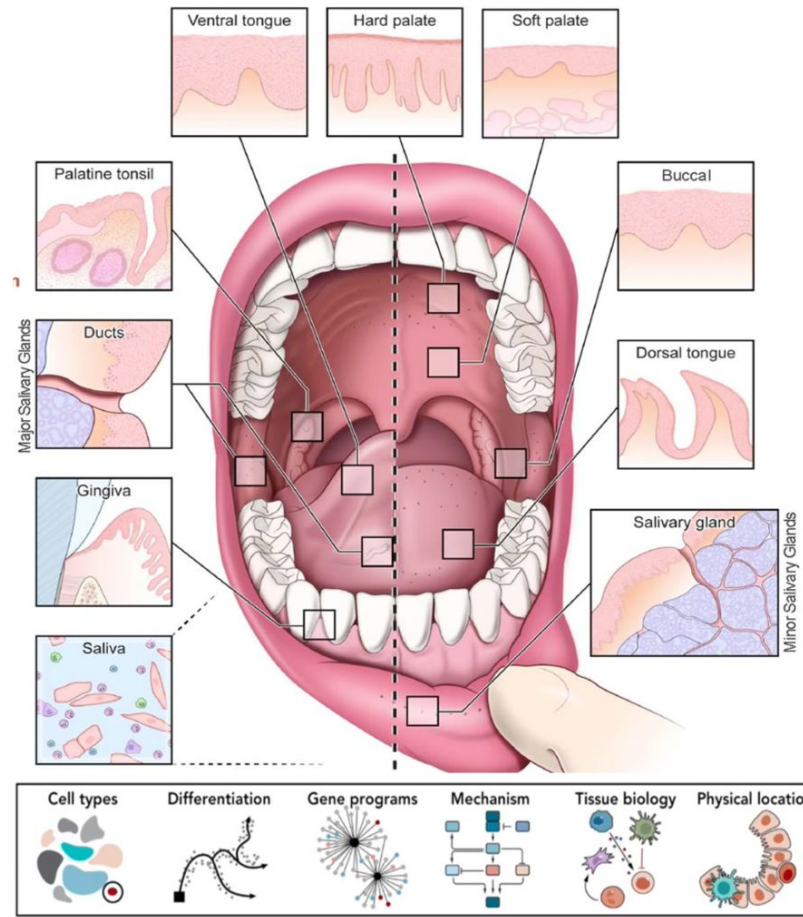
Aphthous Ulceration



Candidiasis



Cell and Molecular Dissection of this Heterogeneity to Promote Health Holistically



References.

Translating Data Into Clinical Insights for Infectious, Autoimmune, and Cancer

nature communications



Article

<https://doi.org/10.1038/s41467-024-49037-y>

Single-cell and spatially resolved interactomics of tooth-associated keratinocytes in p

TITLE: GZMK+CD8+ T cells Target A Specific Acinar Cell Type in Sjögren's Disease

AUTHORS:

Thomas J.F. Pranzatelli^{1,2}, Paola Perez², Anson Ku⁴, Bruno Matuck⁵, Khoa Huynh⁶, Shunsuke Sakai⁷, Mehdi Abed³, Shyh-Ing Jang³, Eiko Yamada³, Kalie Dominick³, Zara Ahmed³, Amanda Olive³, Rachael Wasikowski⁹, Quinn T. Easter³, Alan N. Baer¹⁰, Eileen Pelayo¹⁰, Zohreh Khavandgar^{3,10}, David E. Kleiner¹¹, M. Teresa Magone¹², Sarthak Gupta^{3,13}, Christopher Lessard¹⁴, Robert J. Morelli¹⁵, Changyu Zheng¹⁴, Nicholas Rach¹⁶, Aure¹⁸, Mohammad H. Derfulan¹⁹, Ross Lake²⁰, Sa Sowalsky⁴, Katarzyna M. Tyc⁵, Jinze Liu⁶, Johann G Chiorini¹, Blake M. Warner^{3,10*}

Spatial Deconvolution of Cell Types and Cell States at Scale Utilizing TACIT

Khoa L. A. Huynh^{*,}, Katarzyna M. Tyc^{1,2*}, Bruno F. Matuck^{3*}, Quinn T. Easter³, Aditya Pratapa⁴, Nikhil V. Kumar³, Paola Pérez⁵, Rachel Kulchar⁵, Thomas Pranzatelli⁶, Deiziane de Souza⁷, Theresa M. Weaver³, Xufeng Qu², Luiz Alberto Valente Soares Junior⁸, Marisa Dohnokoff⁷, David E. Kleiner⁹, Stephen M. Hewitt⁹, Luiz Fernando Fer¹⁰, Blake M. Warner⁵, Kevin M. Byrd^{3,5,11*}, Jinze Liu^{1,2#}.

Metacellular Networks and Proteomic Ecotypes Predict Anti-PD-(L)1 Response in HNSCC
Siddharth Sheth^{1,2}, Nikhil Kumar^{3*}, Bruno Matuck³, Khoa Huynh⁴, Allison Deal², John Kaczmar⁵, Bhisham Chera⁵, James Bonner⁶, Jared Weiss^{1,2}, Jinze Liu⁴, Kevin M. Byrd^{4,7}

¹ Department of Medicine, Division of Oncology, University of North Carolina School of Medicine, University of North Carolina School of Medicine, Chapel Hill, NC, USA

² Lineberger Comprehensive Cancer Center, University of North Carolina at Chapel Hill, Chapel Hill, NC, USA

³ Lab of Oral & Craniofacial Innovation, Department of Innovation & Technology Research, ADA Science & Research Institute, Gaithersburg, MD, USA

⁴ Department of Biostatistics, Virginia Commonwealth University, Richmond, VA, USA

⁵ Hollings Cancer Center, Medical University of South Carolina, Charleston, SC, USA

⁶ O'Neal Comprehensive Cancer Center, University of Alabama at Birmingham, Birmingham, AL, USA

⁷ Division of Oral and Craniofacial Health Sciences, University of Maryland School of Dentistry, Baltimore, MD, USA

* Contributed equally

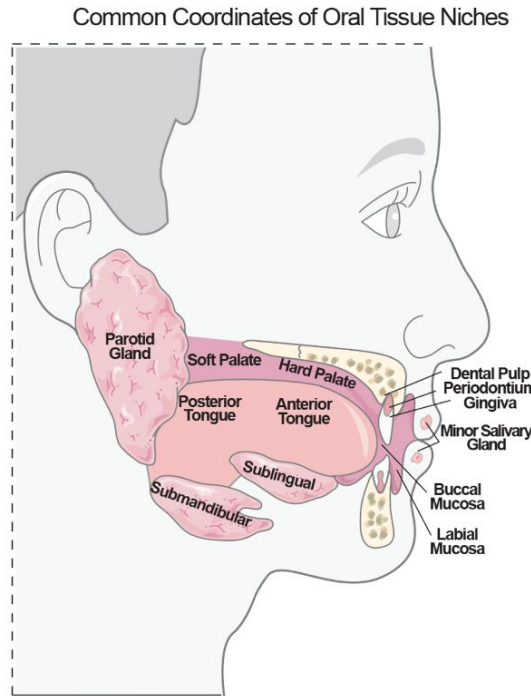
The Immunoregulatory Architecture of the Adult Oral Cavity

Bruno F. Matuck, Khoa L. A. Huynh, Diana Pereira, XiuYu Zhang, Meik Kunz, Nikhil Kumar, Quinn T. Easter, Alexandre Fernandes, Amerre Ghodke, Alexander V. Predeus, Lili Szabó, Nadja Harnischfeiger, Zohreh Khavandgar, Margaret Beach, Paola Perez, Benedikt Nilges, Maria M. Moreno, Kang I. Ko, Sarah A. Teichmann, Adam Kimple, Sarah Pringle, Kai Kretzschmar, Blake M. Warner, Inês Sequeira, Jinze Liu, Kevin M. Byrd

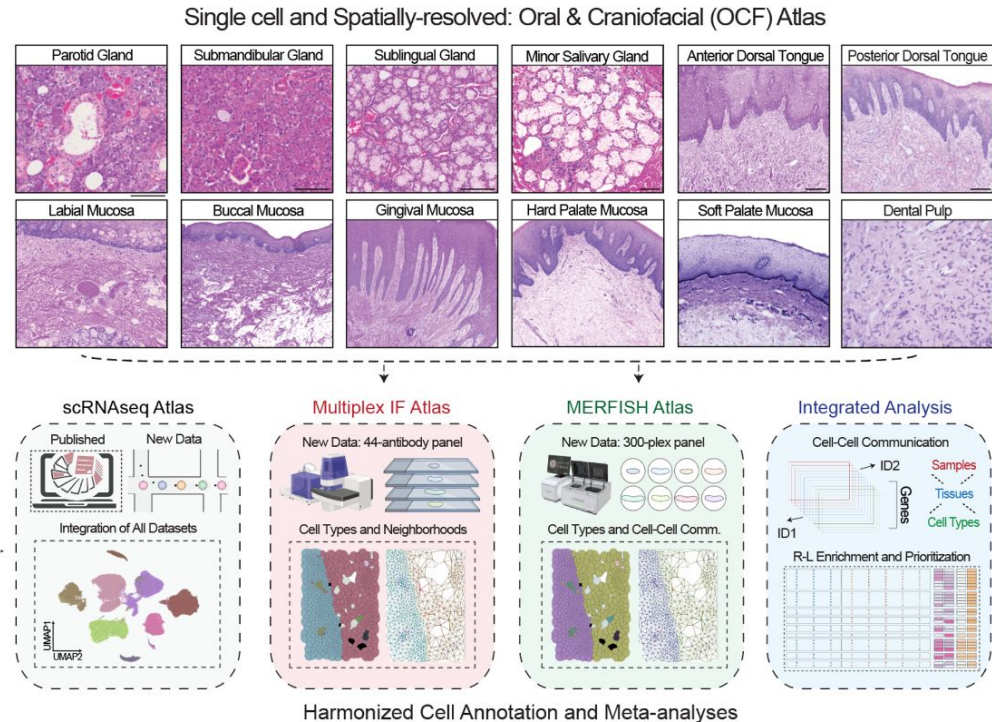
doi: <https://doi.org/10.1101/2024.12.01.626279>

This article is a preprint and has not been certified by peer review [what does this mean?].

P1: Oral & Craniofacial Cell Atlas of Healthy Adults.



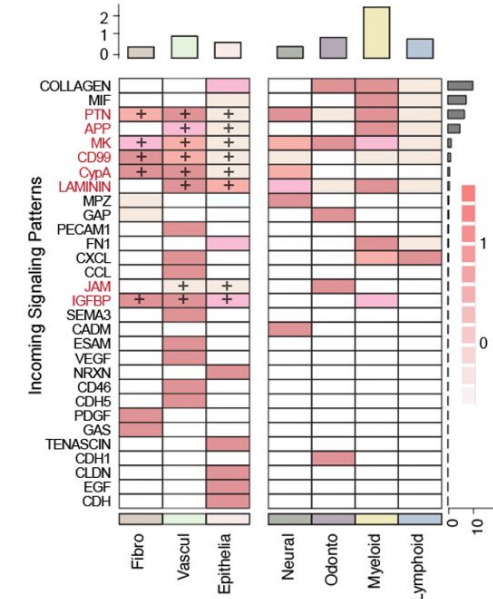
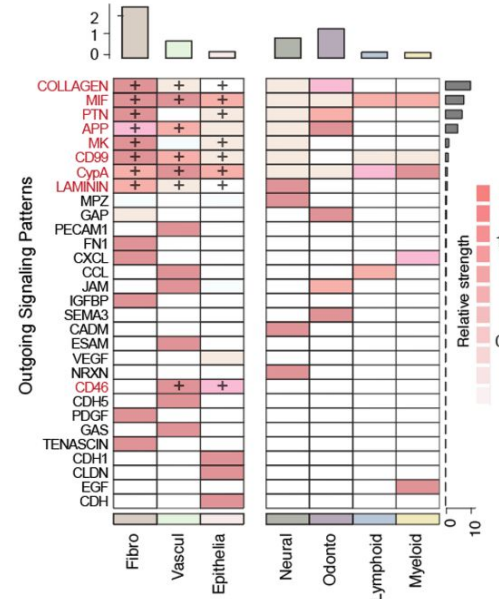
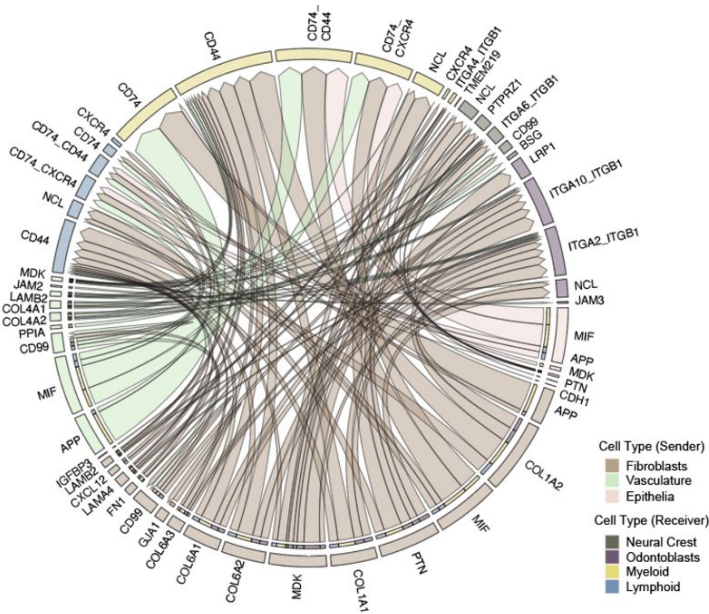
- scRNASeq Studies
- published datasets
- Williams et al.
 - Huang et al.
 - Pagella et al.
 - Costa-da-Silva et al.
 - Krivanek et al.
 - Ko et al.
 - Horeth et al.
 - Caetano et al.
 - Tabula Sapiens
 - Opasawatchai et al.
 - Chen et al.
 - Byrd et al.
 - Pringle et al.
 - Kretschmar et al.
- new datasets



Oral Mucosal Sites Support an Activated Innate Immune Population

P1: Oral & Craniofacial Cell Atlas of Healthy Adults.

Tier 1 Structural and Immune Cell-cell Communication Analysis



Scalable, AI-assisted Cell Identification and Meta-cellular Analyses

AstroSuite: TACIT-Constellation-STARComm-Astrograph: Flexible for Any CELLxFEATURE Matrix

Akoya PCF 2.0

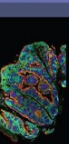


1 Large Sample
300 TMA Cores
Single Run

2 Samples Per Slide
Single Run

1 Large Sample Per Slide
Single Run

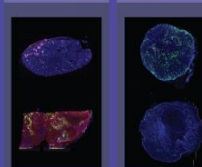
Tonsil



TMA



Skin; Lung

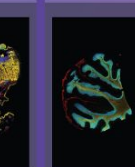


Skin

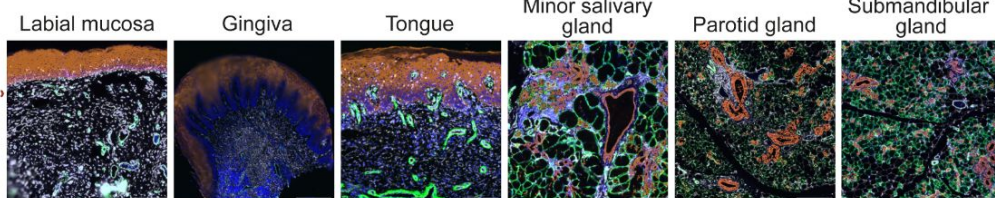
Head & Neck



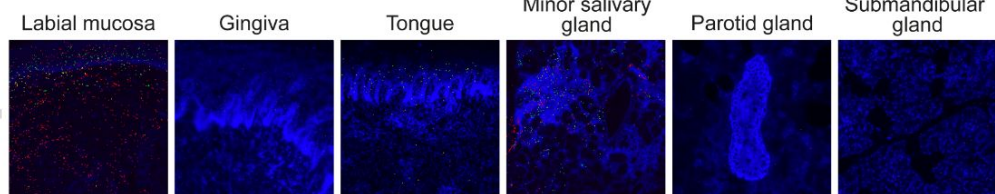
Cerebellum



Phenocycler Fusion



MERSCOPE



Scalable, AI-assisted Cell Identification and Meta-cellular Analyses

Interactive cell type annotation in spatial omics

Choose Signature

Browse... No file selected

Choose slide with annotation

Browse... No file selected

Select samples

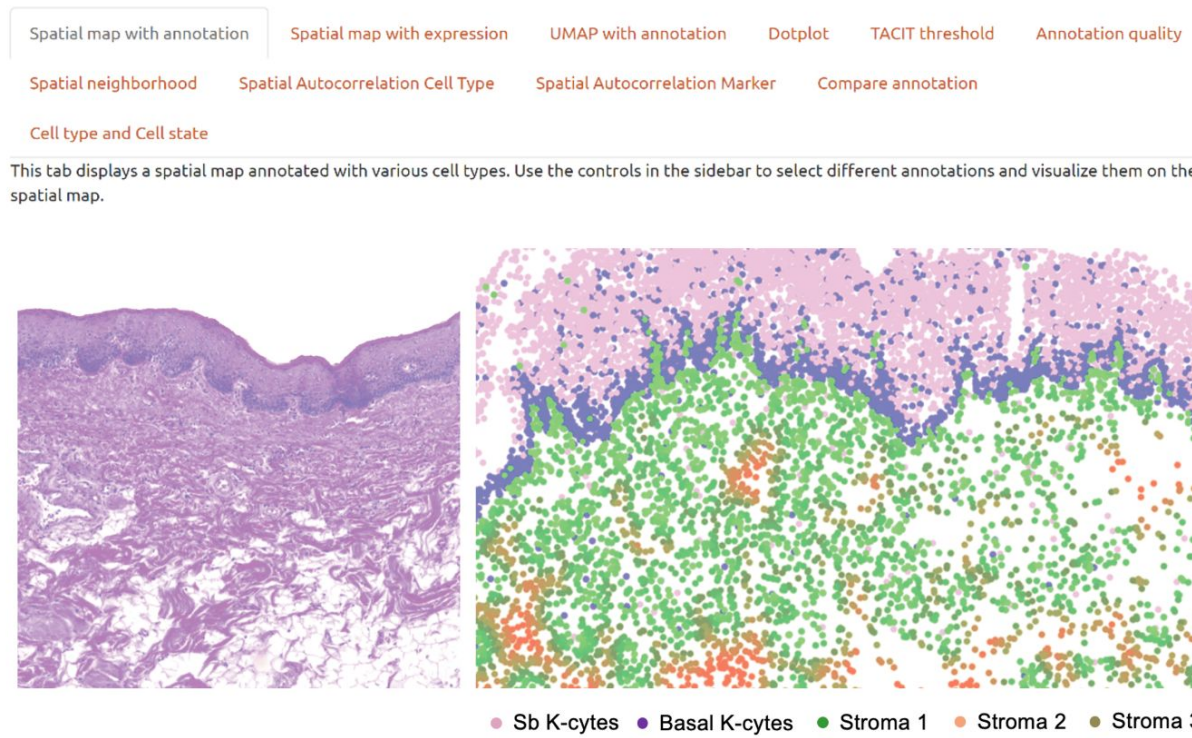
Select annotation

Select Point Size

0.1 0.5 2
0.1 0.3 0.5 0.7 0.9 1.1 1.3 1.5 1.7 1.9 2

Select Cell Type

Select All Deselect All



Oral & Craniofacial Cell Atlas of Healthy Adults: Spatial Proteomics

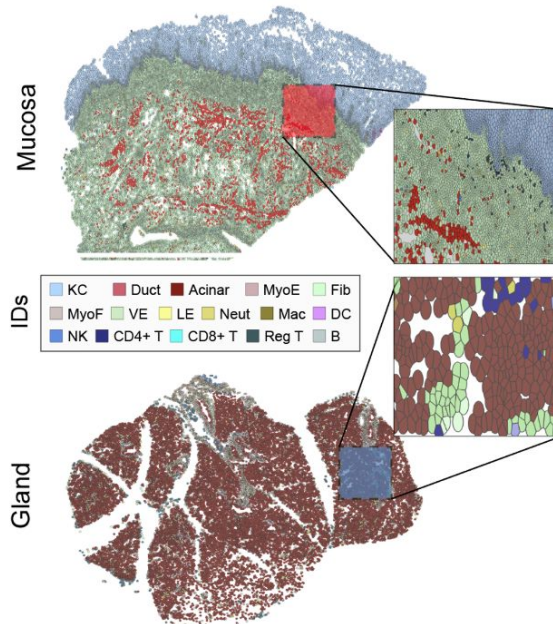
40-plex Multiplex-IF of Immune Cell Populations and States Across Mucosal and Gland Niches

a

scRNASeq	2	KCs	Ductal	Acinar	Iono	Myoepi	Merkel	Fibro	VEC	Mural	LEC	Melano	Schwann	Neuron	Odontoblast	Skeletal Myo	Neutrophils	Mono-Mac	Dendritic Cells	Langerhans	Mast	NK Cells	CD4 T Cells	CD8 T Cells	B Cells	Plasma Cells
multi-IF	2	KCs	Ductal	Acinar	Myoepi	Fibro	Myofibro	VEC	LEC			Neutrophils			Mono-Mac	Dendritic Cells	NK Cells	CD4 T Cells	CD8 T Cells							B Cells

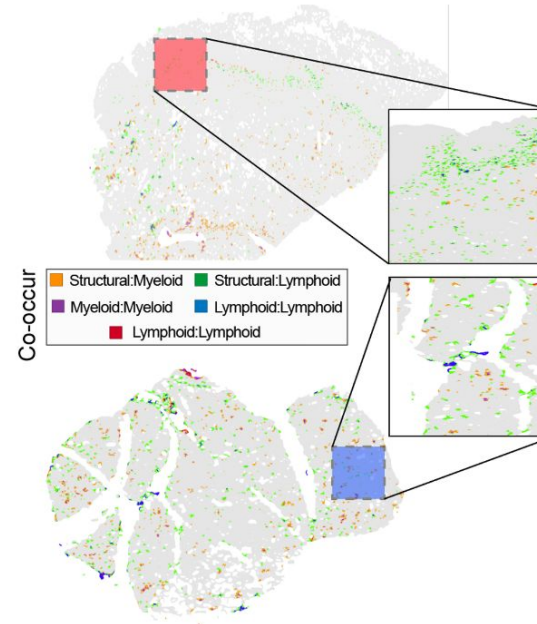
b

Deep Learning Tool for Cell ID (TACIT)



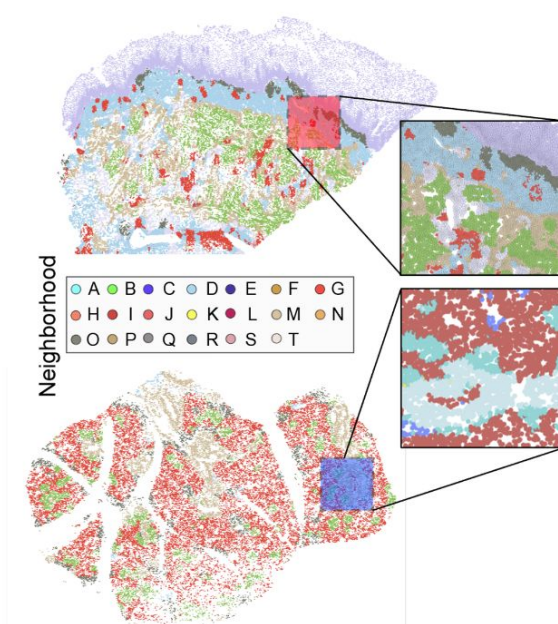
c

Tier 1 Cell Type Co-occurrence

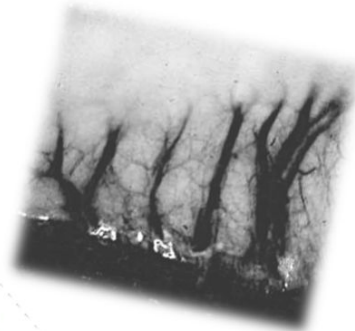
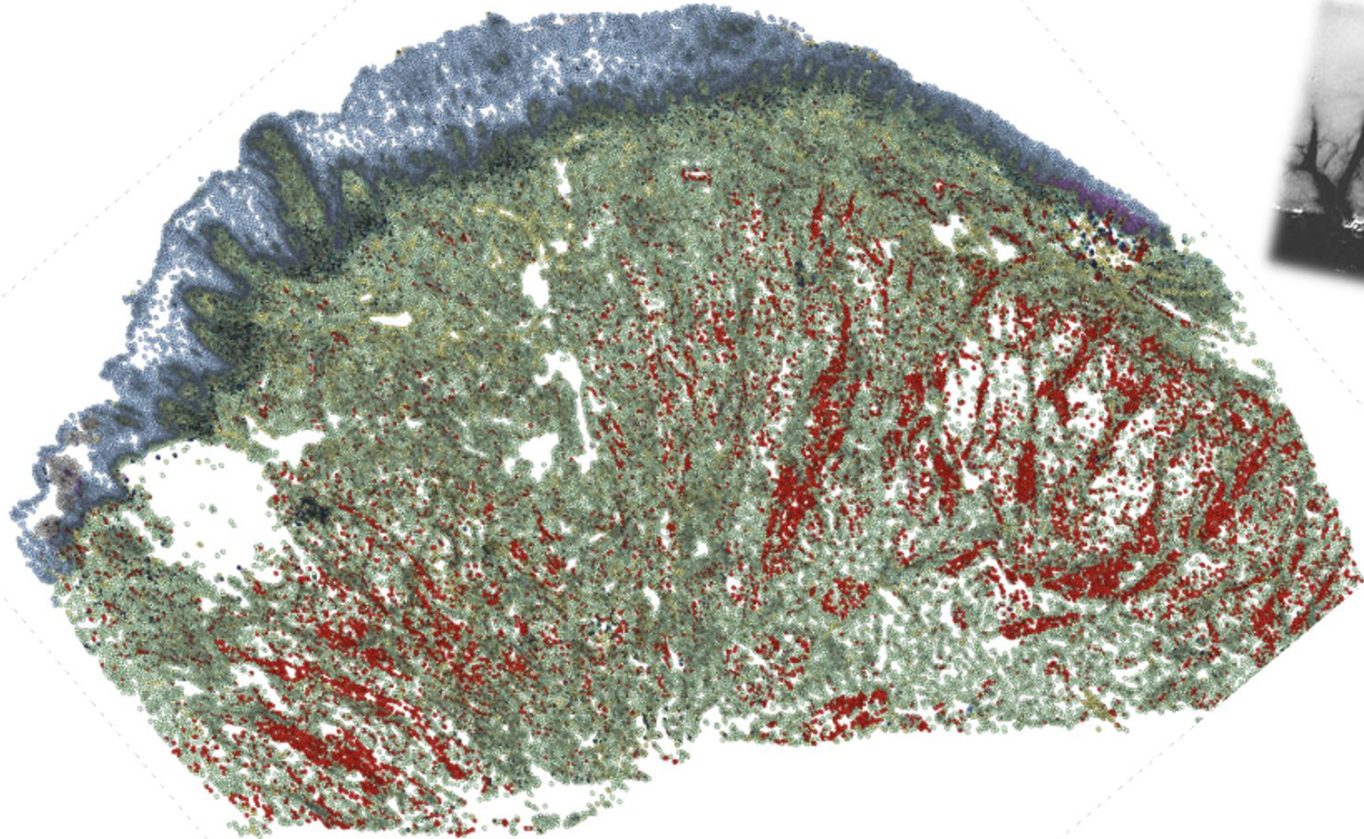


d

Cell Type-Defined Neighborhoods (20)

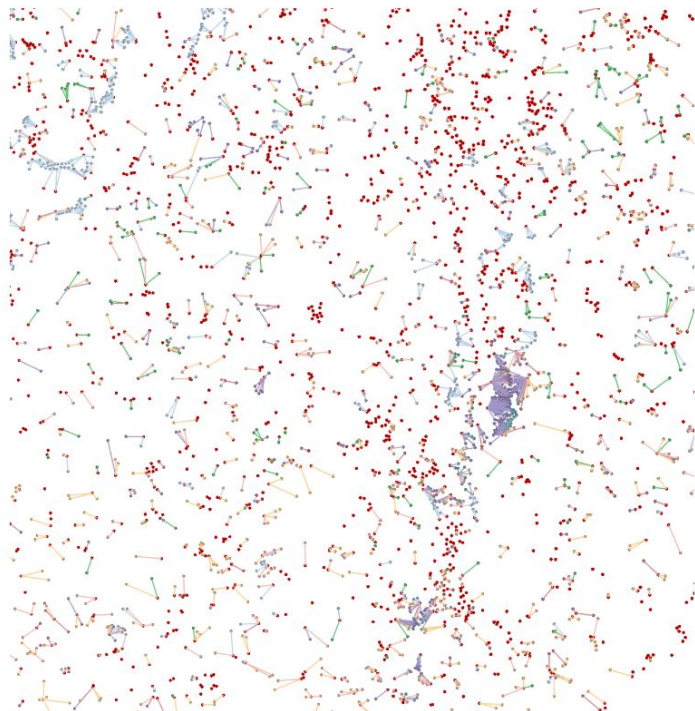


Digitizing the Peripheral Vasculature within Whole Tissues

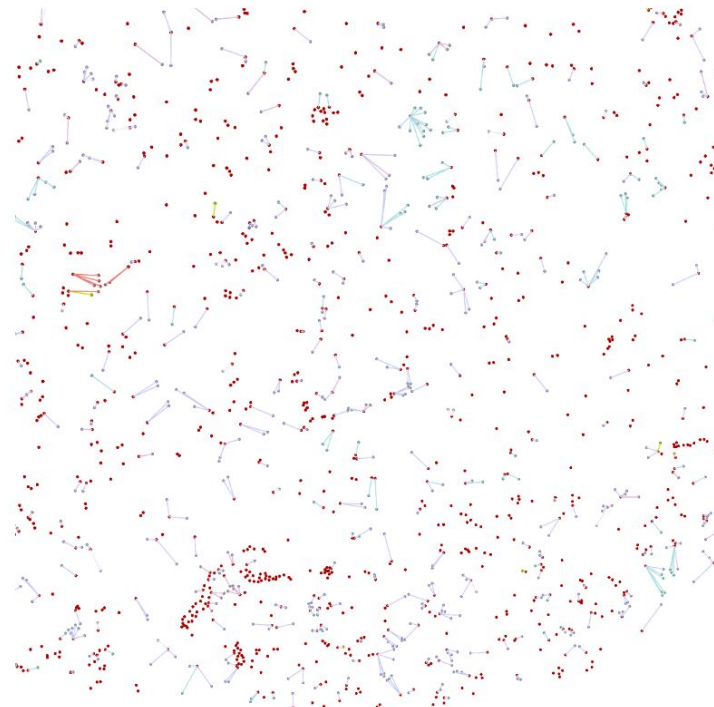


Vascular Anchors for Cell Type Distribution Across Oral Tissues.

Submandibular Salivary Gland



Buccal Mucosa (Cheek)



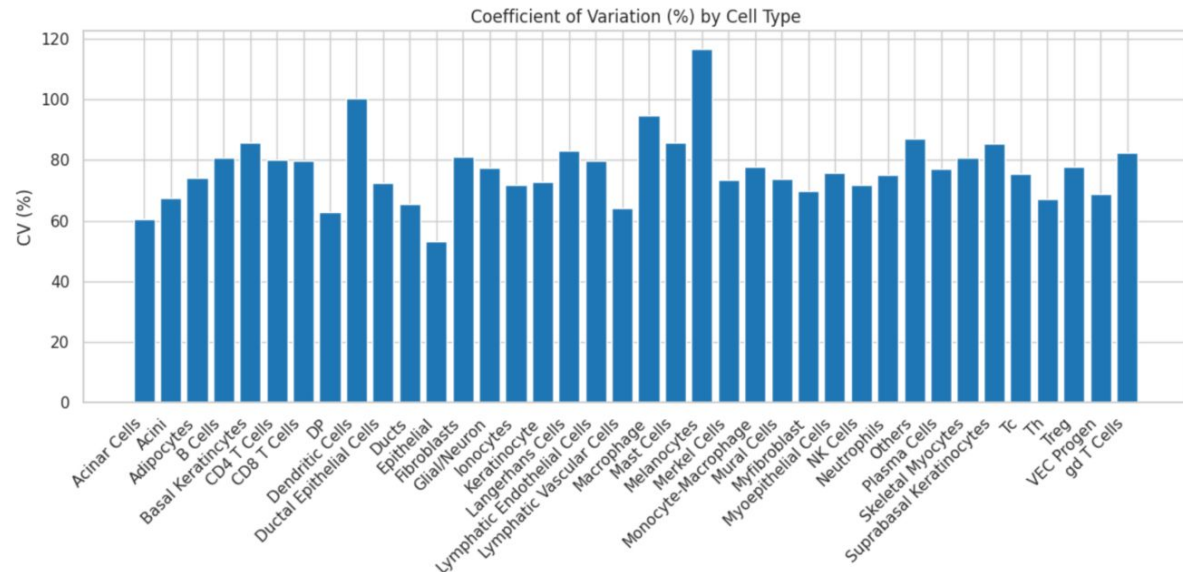
- Fibroblast
- Epithelial
- Endothelial
- Neutrophil
- B cells
- DC cells
- LECs
- NK cells
- Macrophage
- Treg
- Tc
- Th

Variation and Heterogeneity using Vascular Anchors Among Oral Tissues

CV (Coefficient of Variation) is a standardized measure of dispersion of a distribution. (which cell types or regions have more relative variability regardless of their absolute distances)

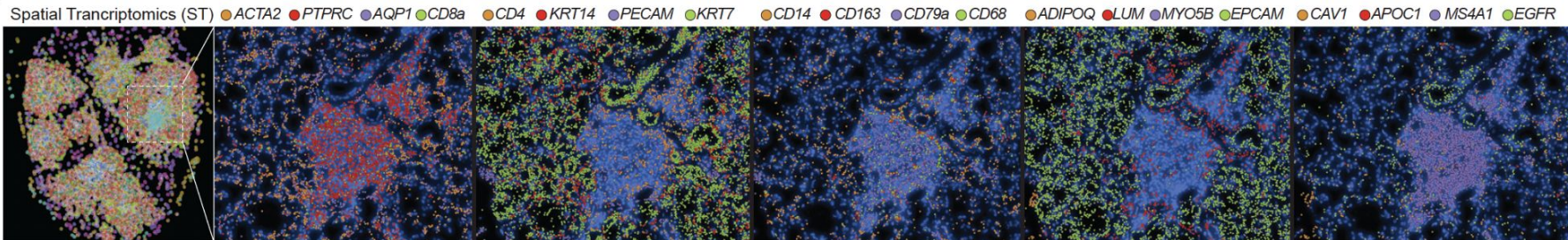
For Region variability, Parotid shows the highest variability in median distances.

For Cell Type variability, Melanocytes and Dendritic Cells show the highest variability.

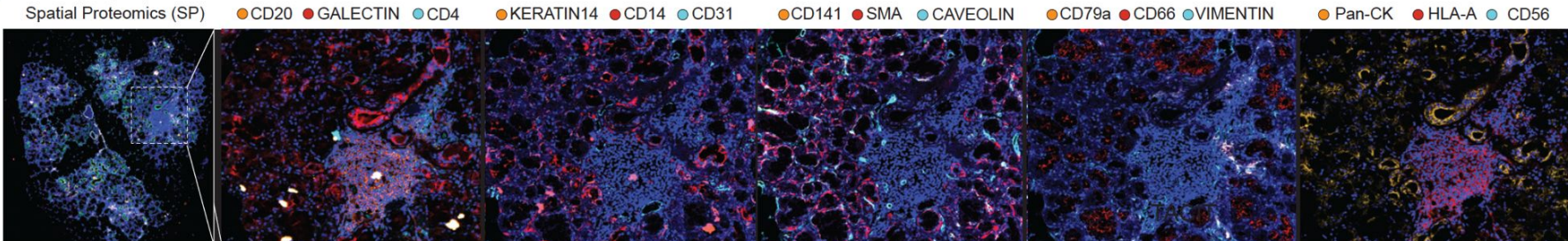


Vascular Anchors for Cell Type Distribution, comparing Spatial Transcriptomics and Proteomics

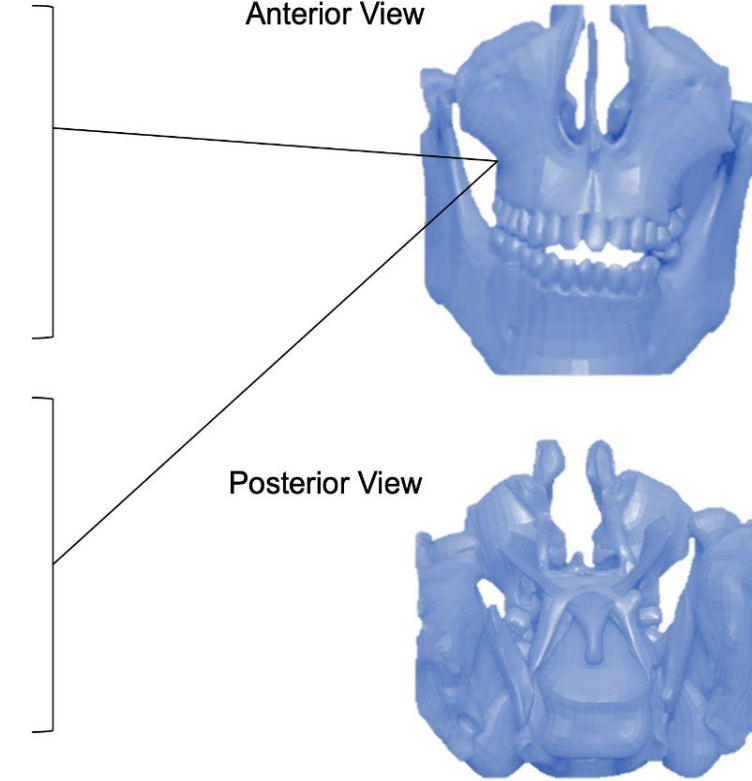
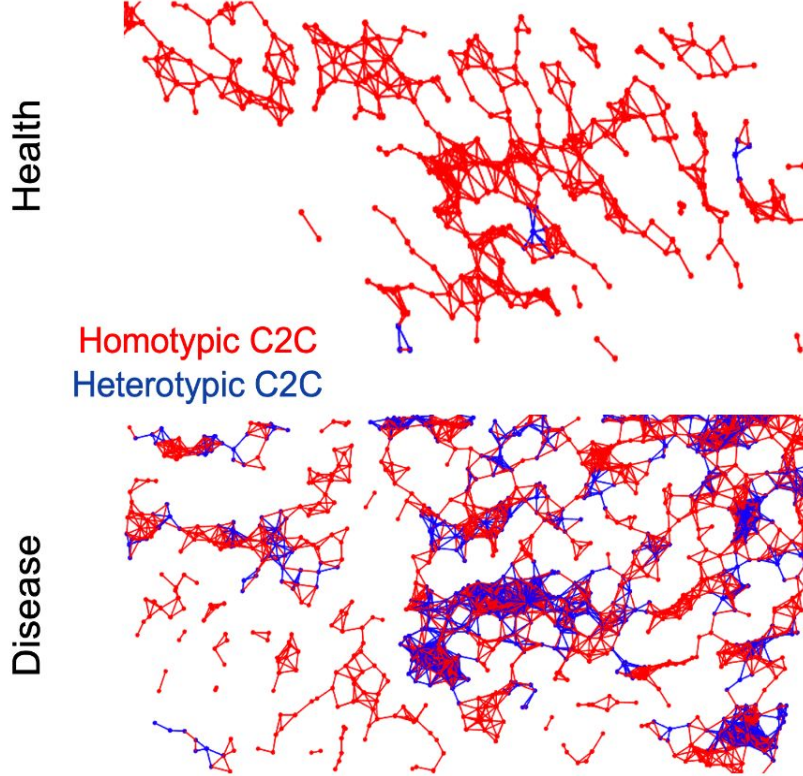
a



b



Vascular Anchors for Cell-Cell Communication.



*****Spatial Health + Disease Atlas:** ~2000 samples with ~50,000,000 cells across 10 upper airway niches and 13 diseases from health to various conditions such as periodontitis, Sjogren's, COVID-19, and multiple cancers.

Thank You.



Lab of Oral & Craniofacial Innovation (LOCI)

- Quinn Easter
- Bruno Matuck
- Terrie Weaver
- Akira Hasuike
- Nikhil Kumar
- Brittany Rupp
- Zabdiel Alvarado-Martinez
- Lijiang Fei

Human Cell Atlas Oral & Craniofacial Bionetwork

- Ines Sequeira
- Ana Caetano
- Kai Kretzschmar
- Adam Kimple
- Muzz Haniffa
- Michel Koo
- Sarah Pringle
- Many Others...

Salivary Disorder Unit (NIH/NIDCR)

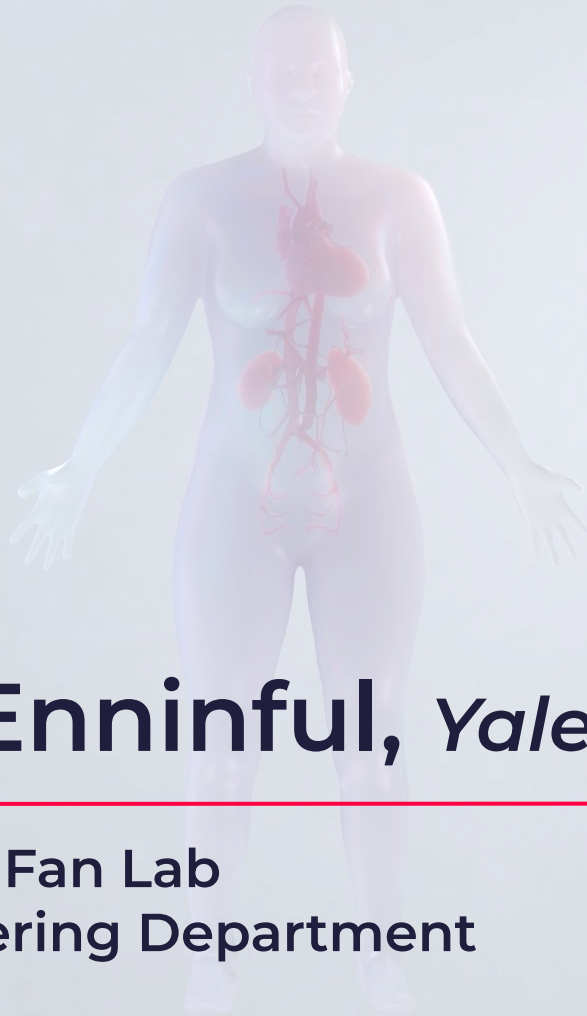
- Blake M. Warner
- Shyh-Ing Jang
- Thomas Pranzatelli
- Paola Perez

Department of Biostatistics (Massey/VCU)

- Jinze Liu
- Katarzyna Tyc
- Khoa Huynh
- Xufeng Qu

Mapping the Pediatric Inhalation Interface Network

- Jim Hagood
- Ric Boucher
- Fabian Theis
- Purushothama Tata
- Herbert Schiller
- Arjun Guha
- Mandy Bush
- Anne Hilgendorf



Archibald Enninful, Yale University

PhD Student, Rong Fan Lab
Biomedical Engineering Department
Yale University



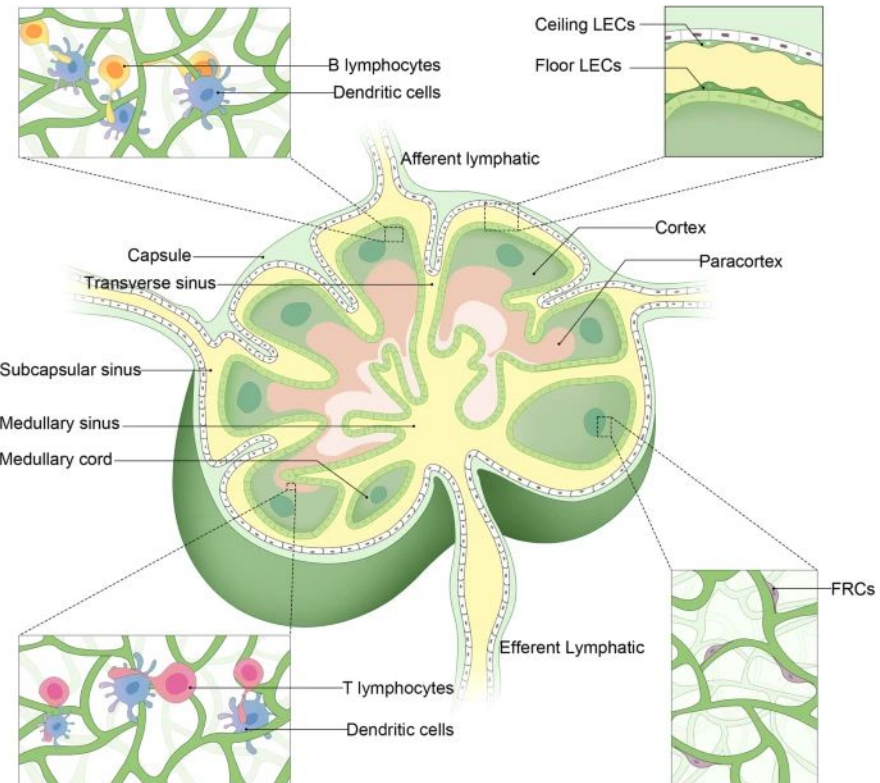
Spatial multi-omics profiling of human lymphoid tissues

Yale HuBMAP TTD

Prof Rong Fan, Prof Yang Liu, Prof George Tellides, Dr. Fu Gao, Dr. Mingyu Yang, Dr. Dongjoo Kim, Archibald Enninful, Negin Farzad, Yao Lu

Overview of Lymph nodes

- The primary lymphoid organs (bone marrow and thymus) are responsible for immune cell production and maturation, whereas secondary lymphoid organs (lymph nodes, spleen, tonsils) are the sites for lymphocyte activation.
- Lymph nodes are found at the convergence of major blood vessels.
- Approximately 800 nodes in an adult human.
- Located in the neck, axilla, thorax, abdomen, and groin.



Lymph nodes samples

33 whole lymph nodes

FFPE samples (**n=16**)

FF samples (**n=17**)

**Lymph node taken from
multiple sites in the body:**

- Axillary
- Inguinal
- Groin
- Submental
- Neck

Primary assay used is mIF (CODEX)

Sample	FF/FFPE	Age
LN21291	FF	71
LN13560	FF	74
LN6243	FF	78
LN00837	FFPE	86
LN24333	FFPE	66
LN21333	FFPE	25
LN23574	FFPE	34
LN22921	FFPE	55
LN27766	FFPE	52
LN00560	FFPE	25
LN21756	FFPE	22

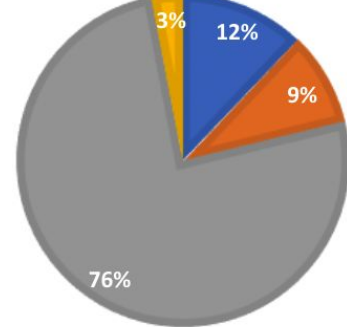
Lymph nodes highlighted in yellow have VCCF visualizations

Lymph nodes samples

<u>Block numbers</u>	<u>Age (yo)</u>	<u>Gender</u>	<u>Location</u>	<u>Race</u>	<u>FF/FFPE</u>
YHLN-N6	63	M	rt inguinal	black	FF
YHLN-N8	29	F	hilar	black	FF
YHLN-N9	54	F	submental	black	FF
YHLN-N17	78	F	lt axillary	black	FF
YHLN-N2	62	M	lt neck	hispanic	FF
YHLN-N22	22	F	lt neck	hispanic	FFPE
YHLN-N27	25	F	right neck	hispanic	FFPE
YHLN-N4	70	M	rt inguinal	pt refused	FF
YHLN-N1	73	F	left groin	white	FF
YHLN-N3	68	M	lt neck	white	FF
YHLN-N5	62	F	left tonsil	white	FF
YHLN-N7	75	F	lt axillary	white	FF
YHLN-N10	1	M	lt neck	white	FF
YHLN-N11	2	M	lt axillary	white	FF
YHLN-N12	20	M	rt neck	white	FF
YHLN-N13	71	F	lt inguinal	white	FF
YHLN-N14	74	M	lt neck	white	FF
YHLN-N15	84	F	rt axillary	white	FF
YHLN-N16	86	M	lt neck	white	FF
YHLN-N18	62	M	rt neck	white	FFPE
YHLN-N19	81	M	rt base of tongue	white	FFPE
YHLN-N20	65	M	right axillary	white	FFPE
YHLN-N21	45	F	lt axillary	white	FFPE
YHLN-N23	50	M	right neck	white	FFPE
YHLN-N24	74	F	right inguinal	white	FFPE
YHLN-N25	74	F	right inguinal	white	FFPE
YHLN-N26	86	M	left axillary	white	FFPE
YHLN-N28	55	M	right neck	white	FFPE
YHLN-N29	34	M	left neck	white	FFPE
YHLN-N30	55	F	left neck	white	FFPE
YHLN-N31	22	M	right axilla	white	FFPE
YHLN-N32	61	M	right groin	white	FFPE
YHLN-N33	63	F	right axilla	white	FFPE

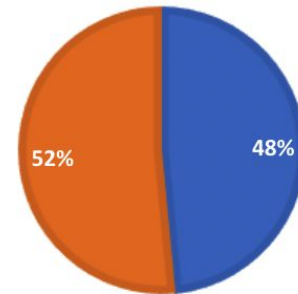
RACE

■ black ■ hispanic ■ white ■ pt refused



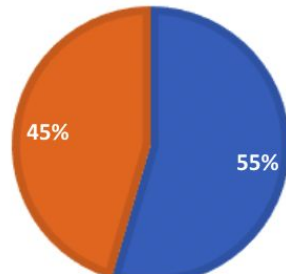
FRESH FROZEN VS FFPE

■ FF ■ FFPE

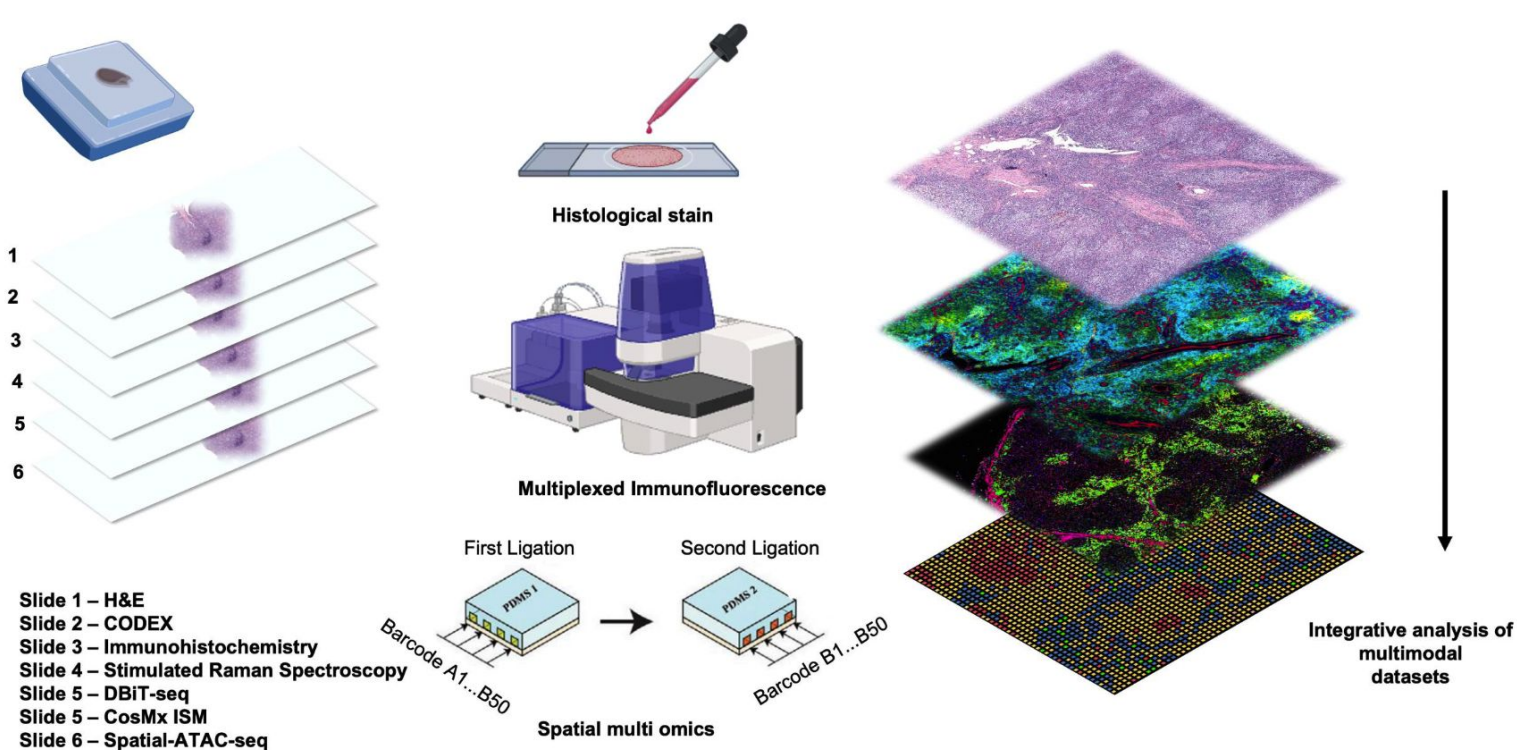


GENDER

■ Male ■ Female



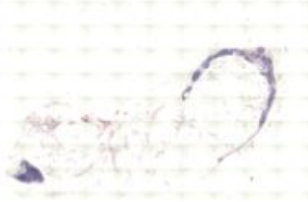
Workflow



Gallery of Lymph nodes samples



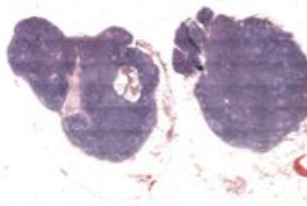
86-year-old
LN-00837 01-01



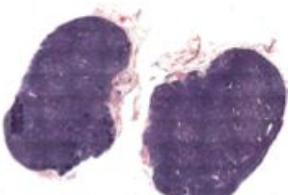
75-year-old
LN-8905 01-04



75-year-old
LN-8905 01-05



66-year-old
LN-24336 01-01



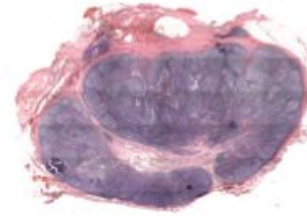
55-year-old
LN-22921 02-01



52-year-old
LN-27766 01-01



34-year-old
LN-23574 03-01



24-year-old
LN-21333 01-01



25-year-old
LN-00560 01-01



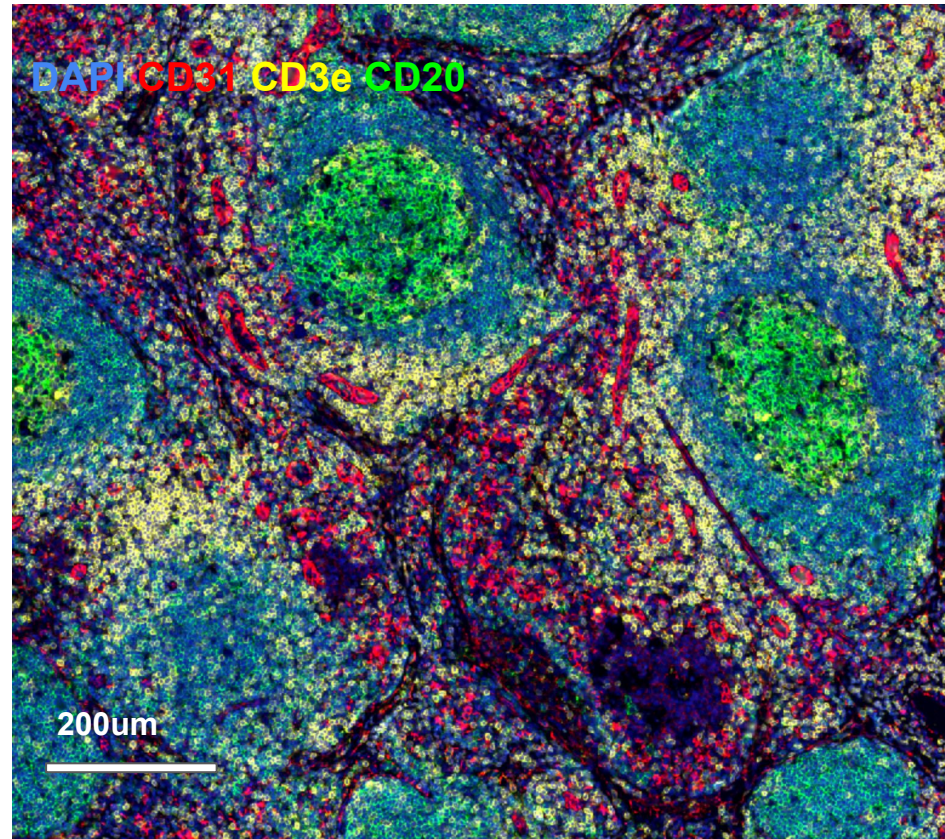
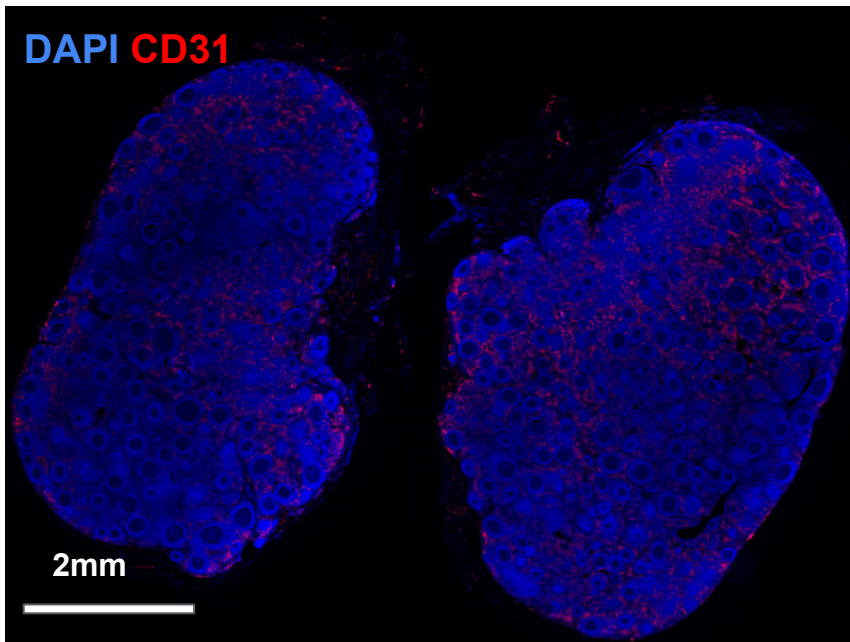
22-year-old
LN-21756 02-01

CODEX Panel

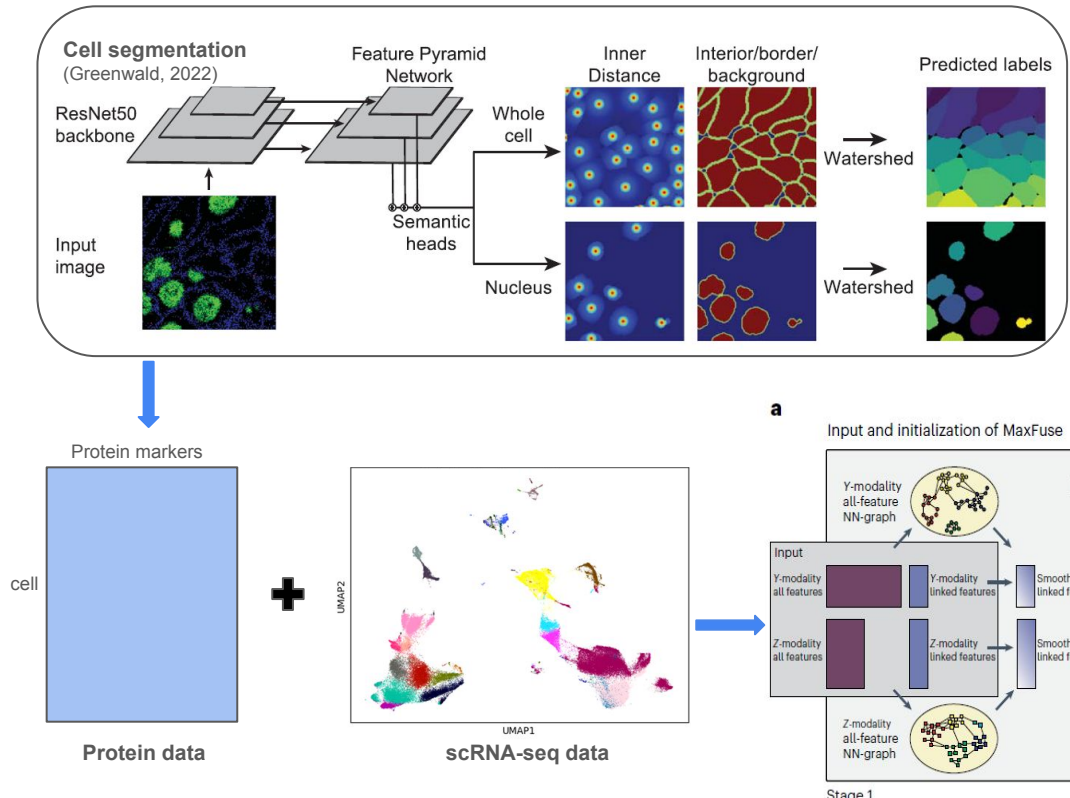
Protein markers covers all the major immune cell types

CD44	SMA	Ki67	CD34	Pan-Cytokeratin
CD31	CD8	CD66	PD1	IDO1
Vimentin	HLA-A	IFN-G	HLA-E	E-cadherin
Collagen IV	CD3e	HLA-DR	LAG3	CD11e
Podoplanin	CD21	Granzyme B	CD14	TOX
CD4	Beta-actin	CD68	CXCR5	<i>HMGB1</i>
CD38	PCNA	CD39	VISTA	<i>yH2AX</i>
CD20	Mac2/Galectin-3	FOXP3	CXCL13	<i>P21</i>
CD107a	EpCAM	MPO	CD163	<i>CDKN2A/p16</i>
CD45RO	CD45	PD-L1	CD141	

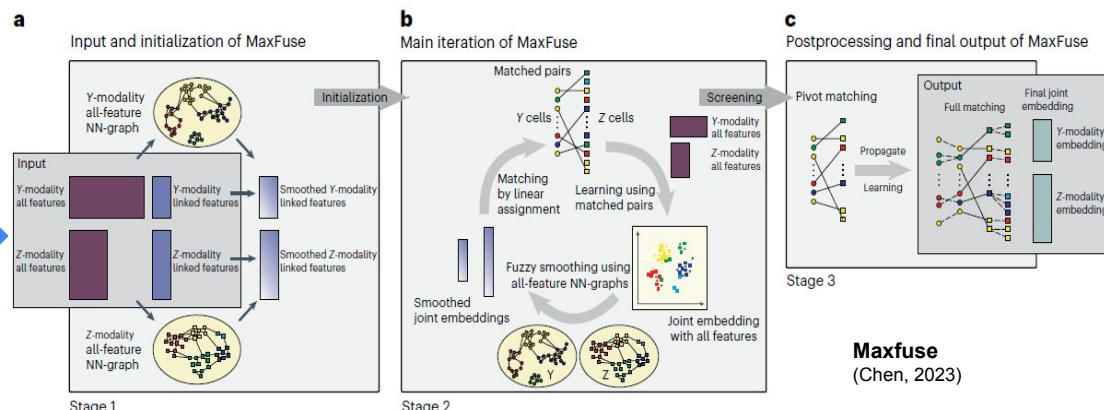
Representative CODEX images



CODEX and scRNA-seq data integration pipeline



We utilize Mesmer, a deep-learning based method, to segment whole cell from CODEX data with the input of both nuclear and membrane markers. After cell segmentation, expression of all protein markers are extracted for each cell. We then use the protein expression along with our reference scRNA-seq data as input to feed into Maxfuse, which finds pairs between CODEX and scRNA-seq data.



We created a human single cell reference by merging two single-cell RNA-seq datasets: **Tabula Sapiens (TS)** and an integrated secondary lymphoid organ (SLO) atlas

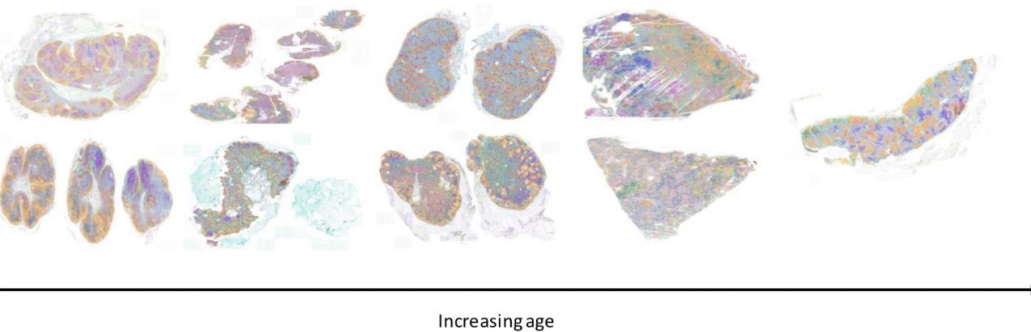
Profiling of Healthy Lymph Nodes using CODEX

A



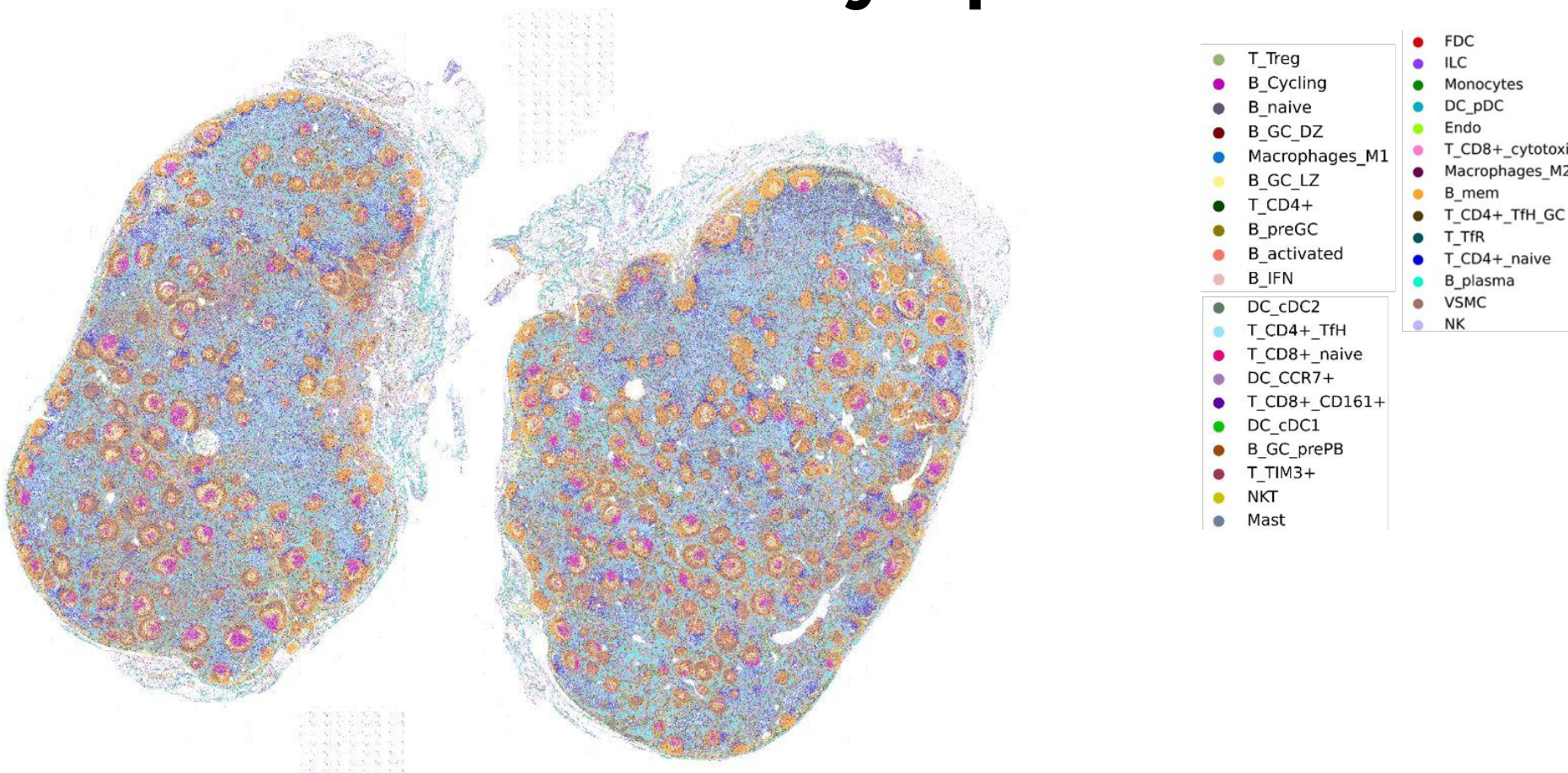
B

Spatial cell type atlas of human lymph nodes across age groups

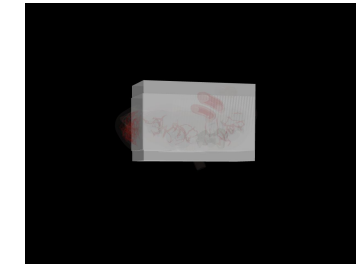
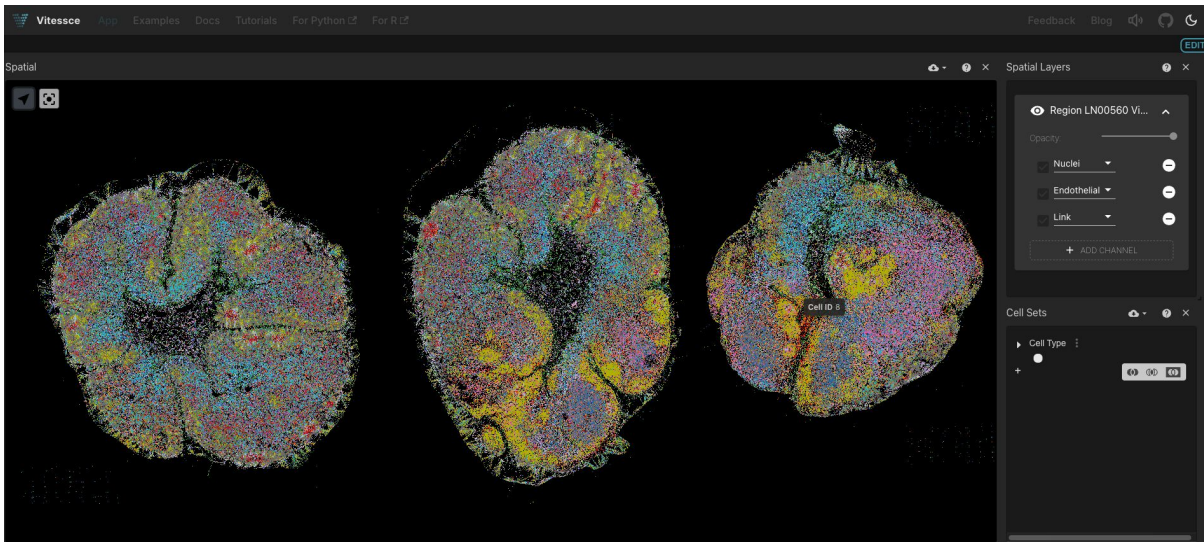


- FDC
- ILC
- Monocytes
- DC_pDC
- Endo
- T_CD8+_cytotoxic
- Macrophages_M2
- B_mem
- T_CD4+_Tfh_GC
- T_Tfr
- T_CD4+_naive
- B_plasma
- NK
- T_Treg
- B_Cycling
- B_naive
- B_GC_DZ
- Macrophages_M1
- B_GC_LZ
- T_CD4+
- B_preGC
- B_activated
- B_IFN
- DC_cDC2
- T_CD4+_Tfh
- T_CD8+_naive
- DC_CCR7+
- T_CD8+_CD161+
- DC_cDC1
- B_GC_prePB
- T_TIM3+
- NKT
- Mast

Annotation of human lymph node



Vascular Common Coordinate Framework Visualizations



Registering tissue block to organ

ACKNOWLEDGEMENTS

Advisor

Professor Rong Fan

Fan Lab members

Negin Farzad	Zhiliang Bai
Alev Baysoy	Anthony Fung
Shuozhen Bao	Haikuo Li
Graham Su	Di Zhang
Xiaoyu Qin	Mei Zhong
Mingyu Yang	Fu Gao
Mingze Dong	Keyi Li
Jungmin Nam	Dongjoo Kim
Bo Tao	Yaping Li
Xiaolong Tian	Fang Wang
Yao Lu	Junchen Yang
	Lou Xing

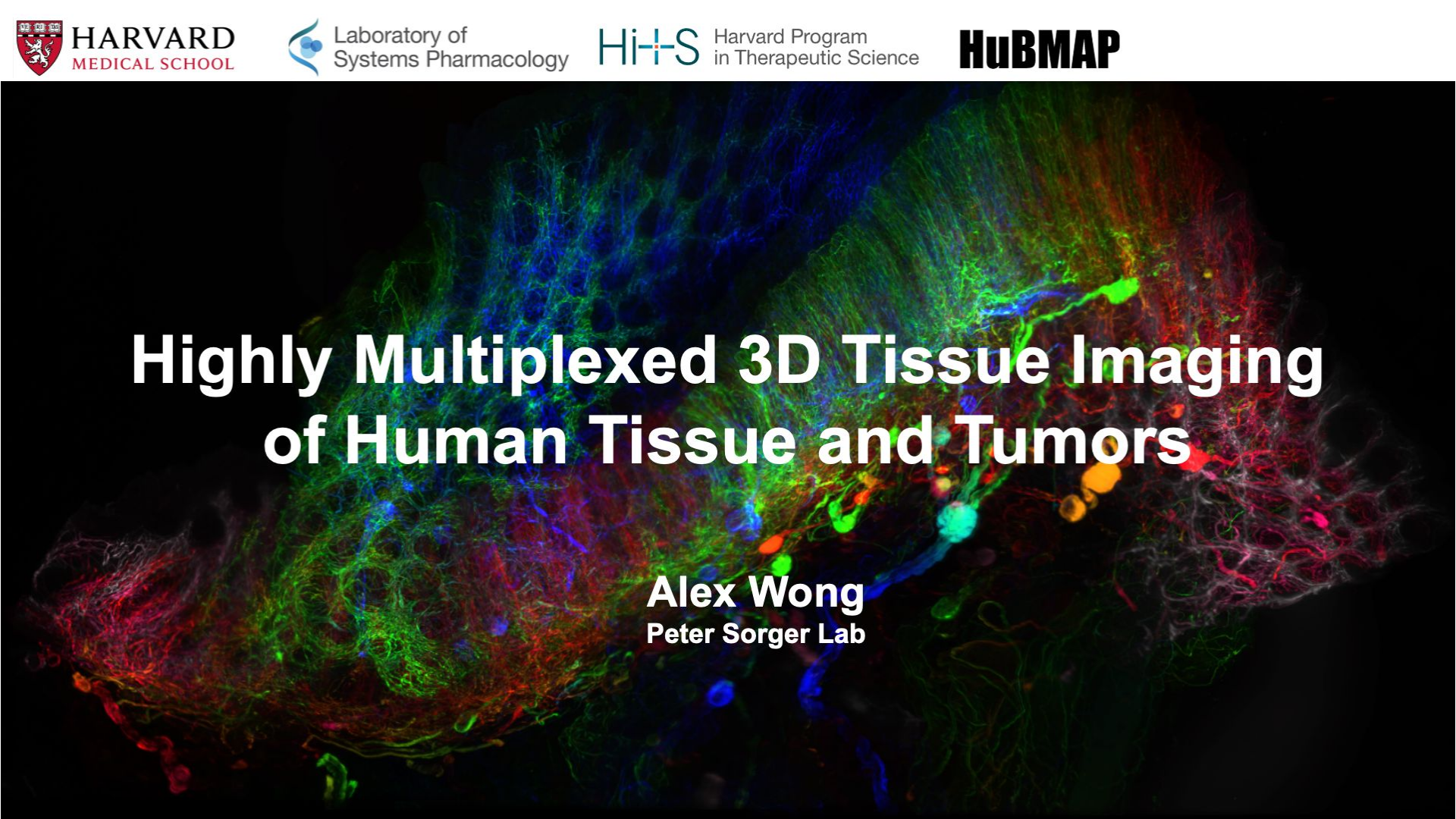
Collaborators

Professor Zongming Ma
Jane Zhang (University of Pennsylvania)
Dmytro Klymyshyn (Akoya Biosciences)
Professor Lingyan Shi (UC San Diego)
Yajuan Li (UC San Diego)





Alex Wong, Ph.D.
Postdoctoral Fellow, Sorger Lab
Harvard Medical School



Highly Multiplexed 3D Tissue Imaging of Human Tissue and Tumors

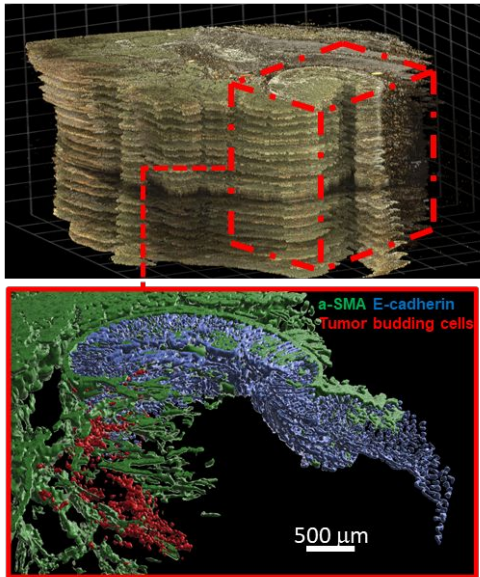
Alex Wong
Peter Sorger Lab

3D Features in Cancer

	Convoluted shapes	Distributions	Sparse features
Features	Nerves, vasculature & Collagen	Spatial relationship of cell types and distance to structures	Rare cell types and structures in 3D volume
Applications	Quantification of cell-structure interactions Measure extent of innervation	Immune surveillance of tumors – Lymphonets Tumor cell distribution	Persistor cells locations-drug studies Perineural Invasion

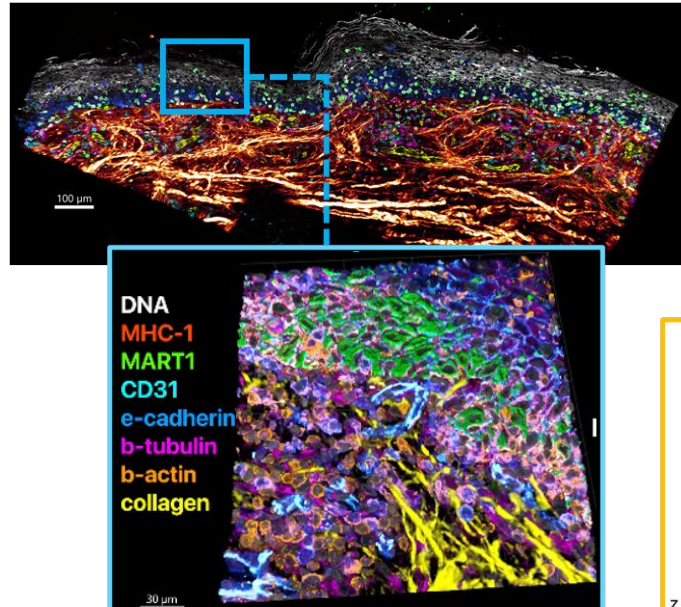
Three Modalities of High-Plex 3D Imaging

1. 3D reconstructive fluorescence microscopy



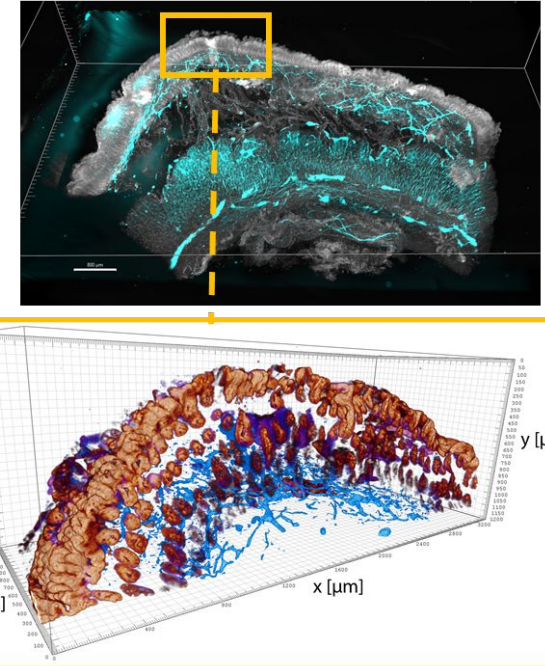
J. Lin et al., Cell, 2023

2. Confocal microscopy / Widefield + Deconvolution



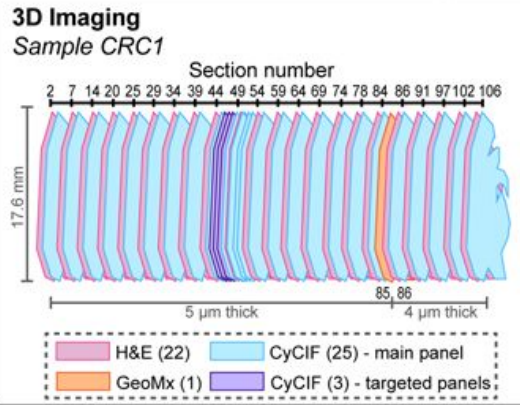
C. Yapp et al., BioRxiv, 2023

3. Light-Sheet Microscopy

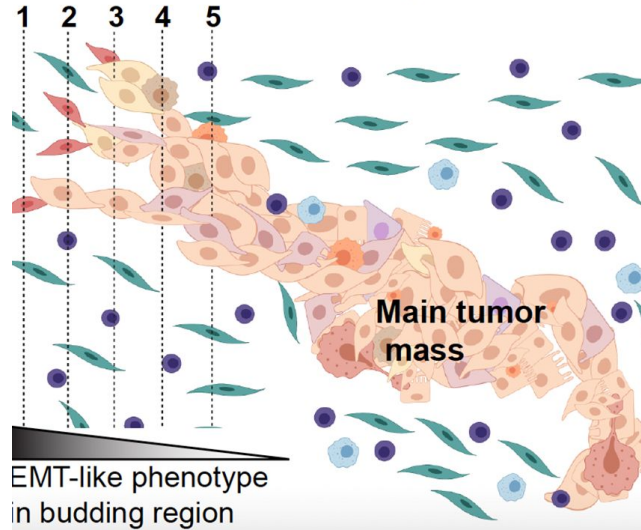


Serial Section Reconstruction

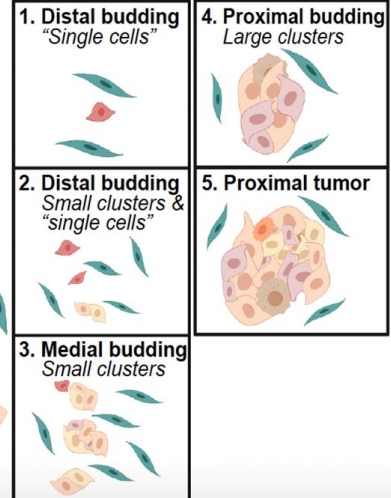
Specimens and data collection strategy



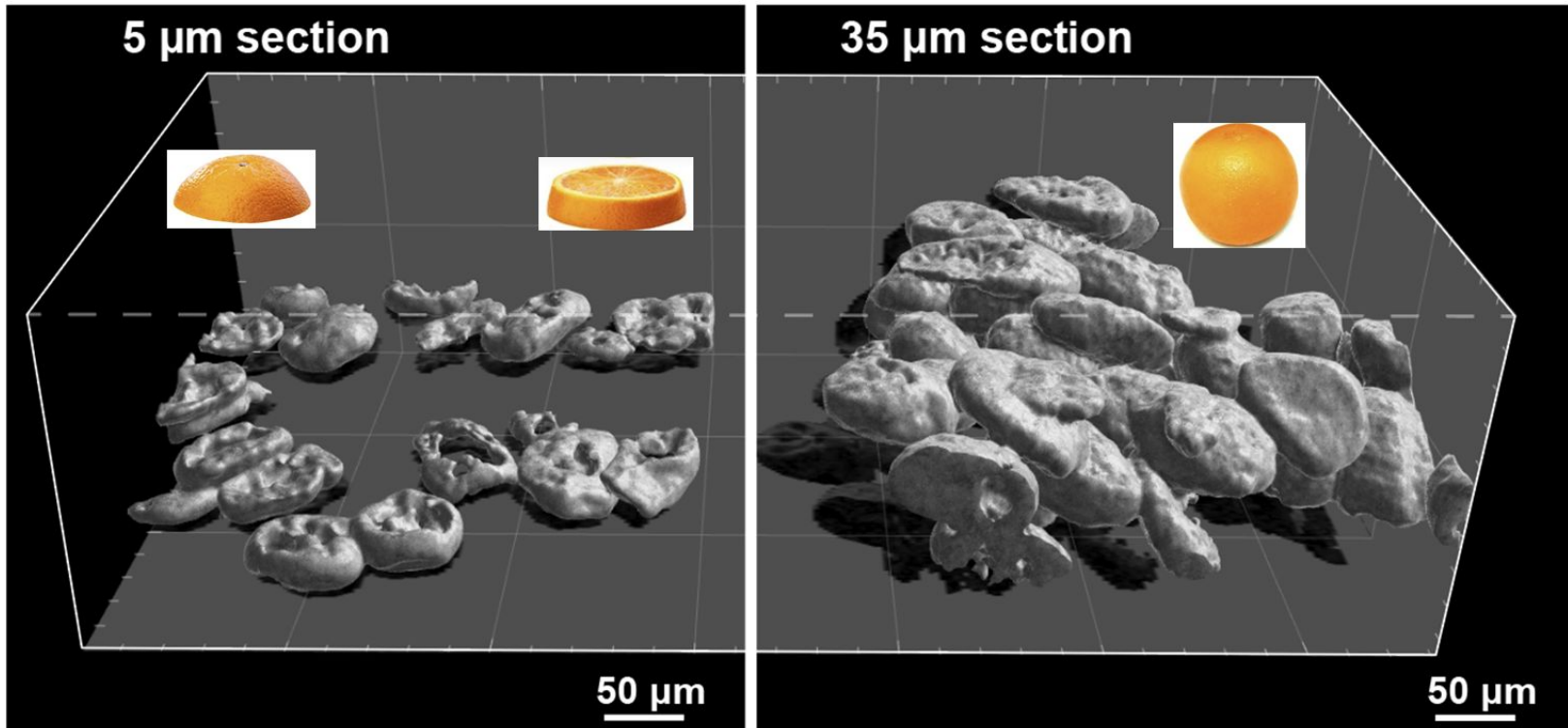
Fibrillar tumor budding



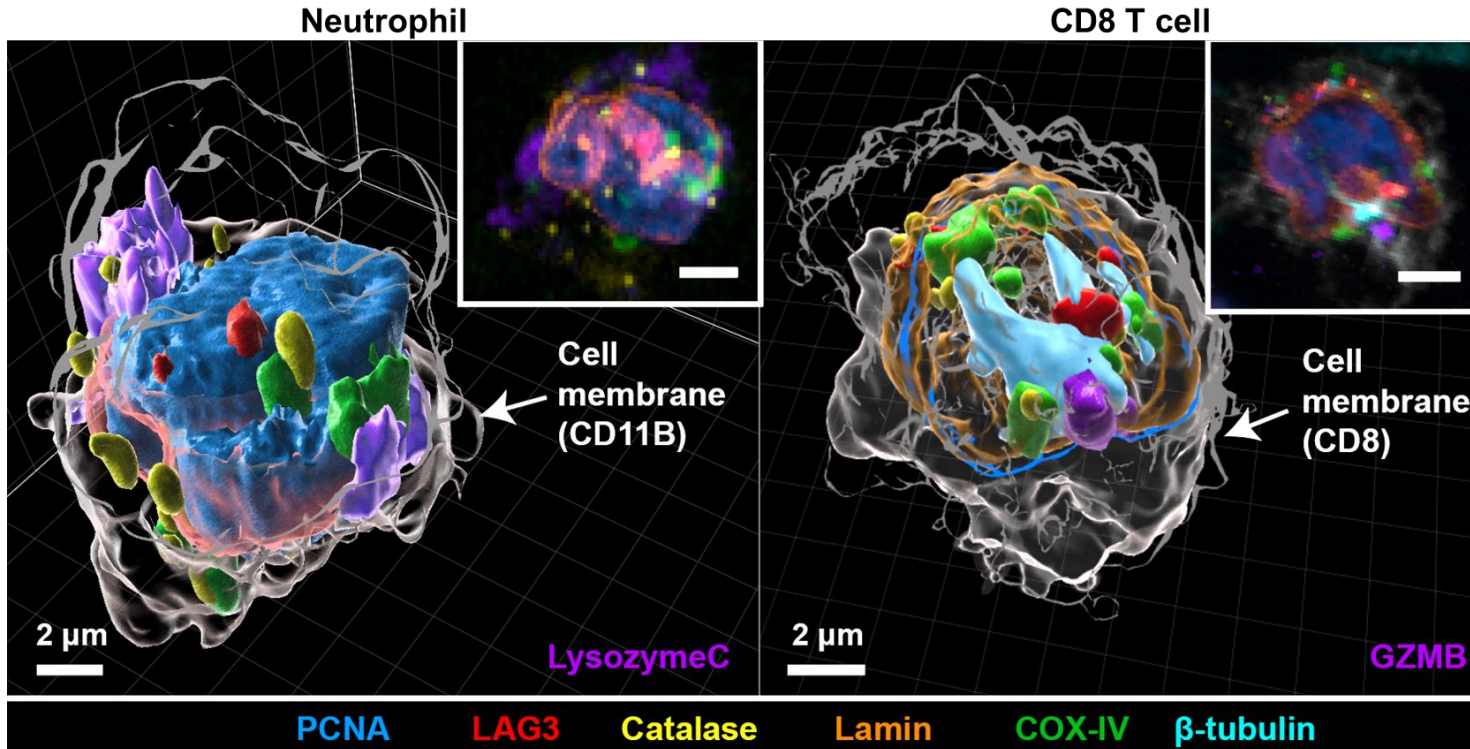
Cross-sectional views



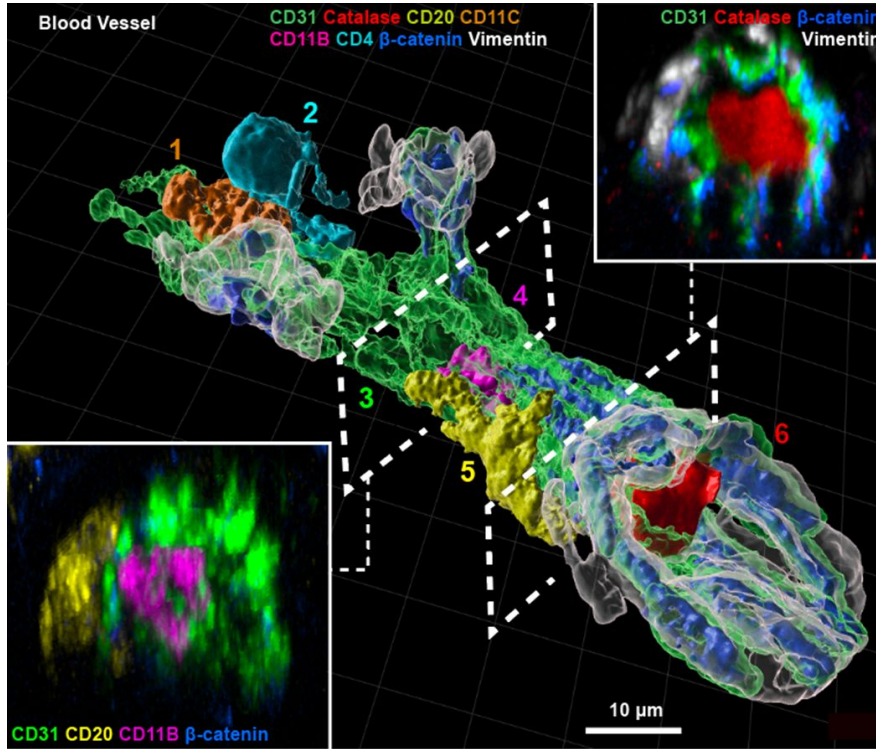
Standard Slides don't even capture whole cells!



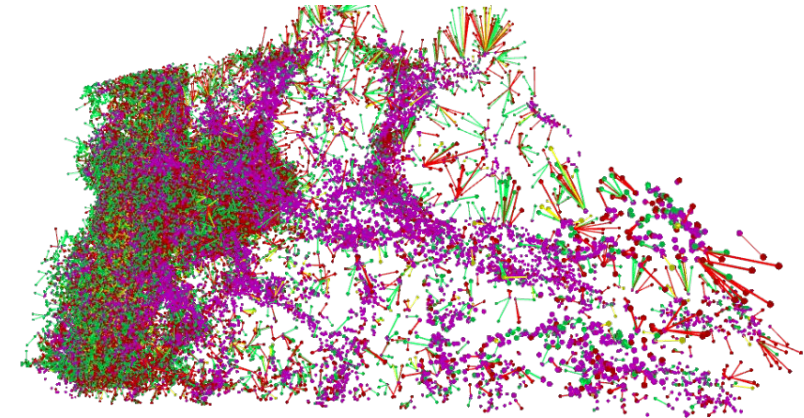
Partial cells lead to inaccurate phenotyping



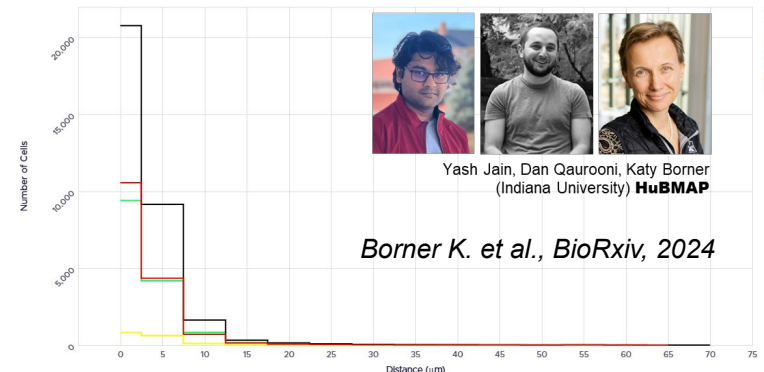
Integrating thick tissue 3D Images into HuBMAP CCF



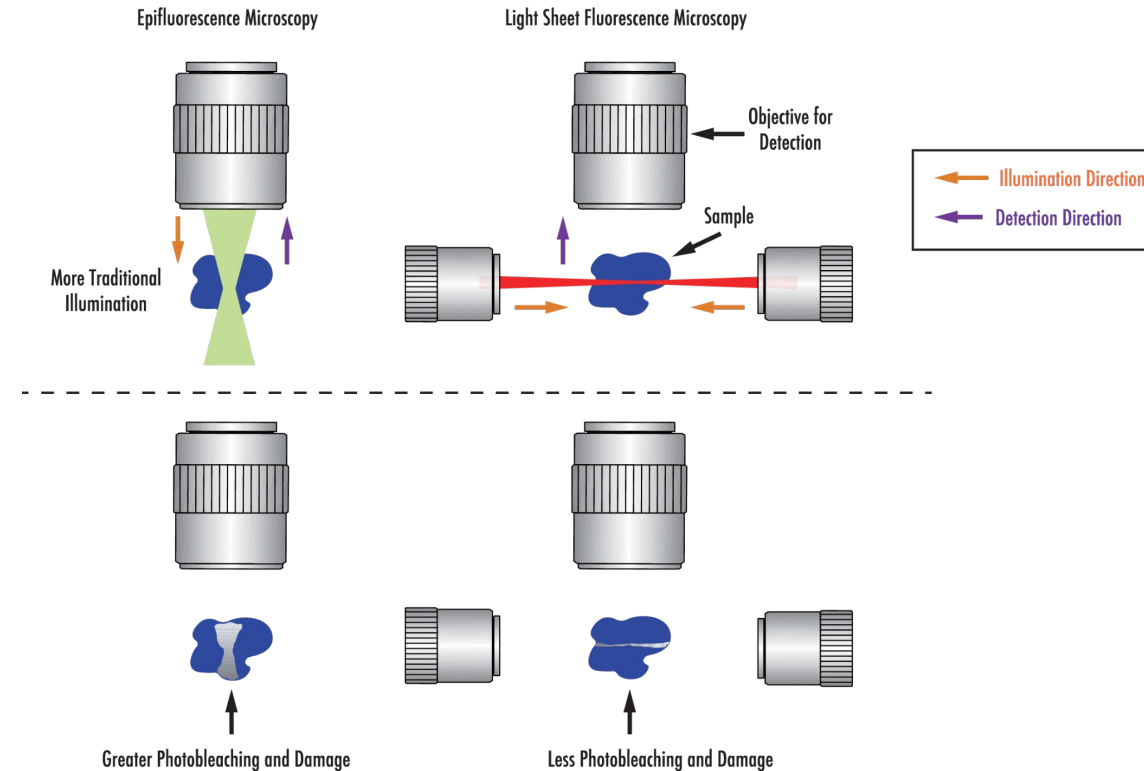
C. Yapp et al., *BioRxiv*, 2023



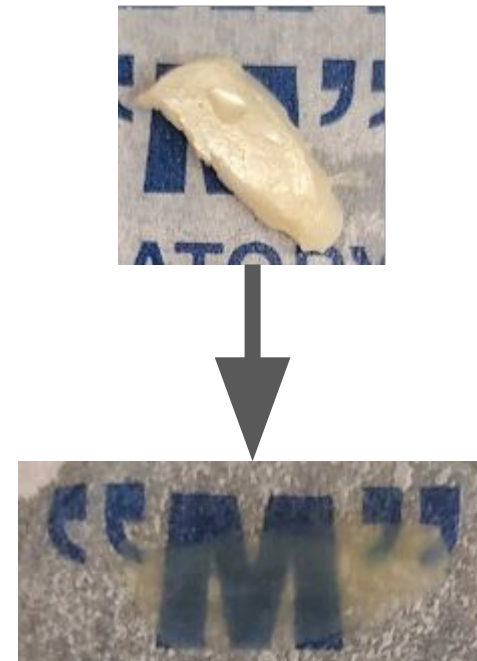
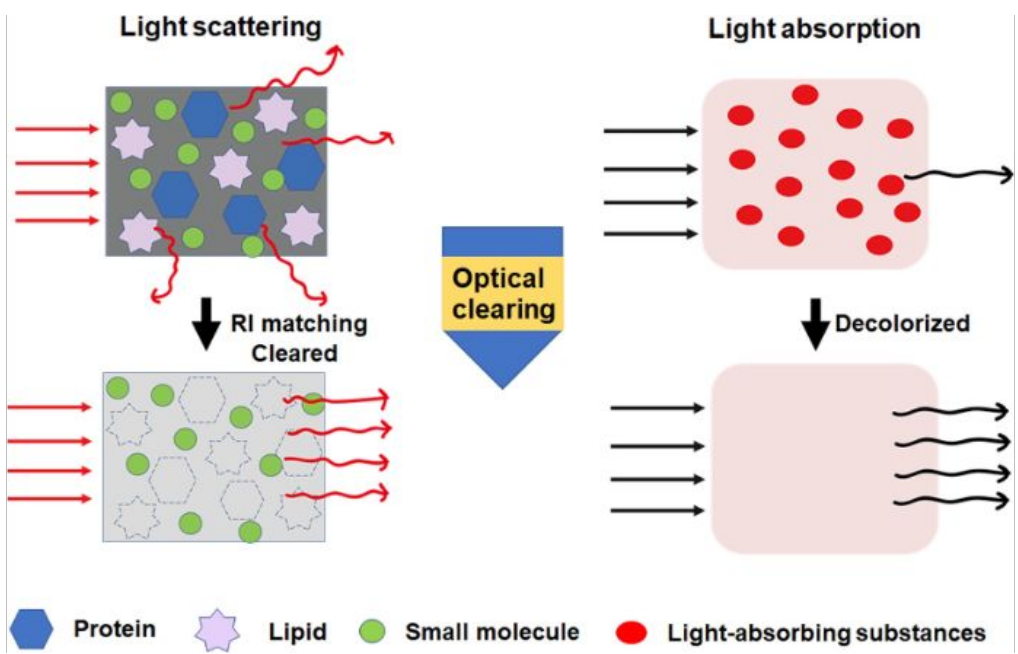
<https://apps.humanatlas.io/cde/example/1>



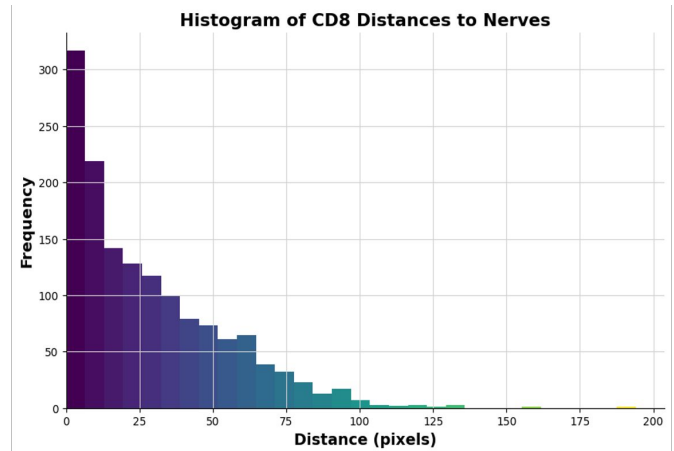
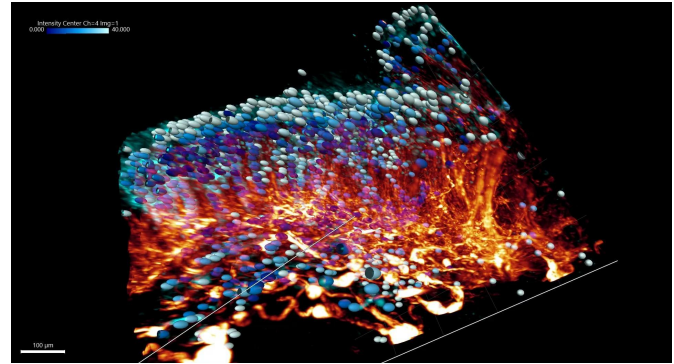
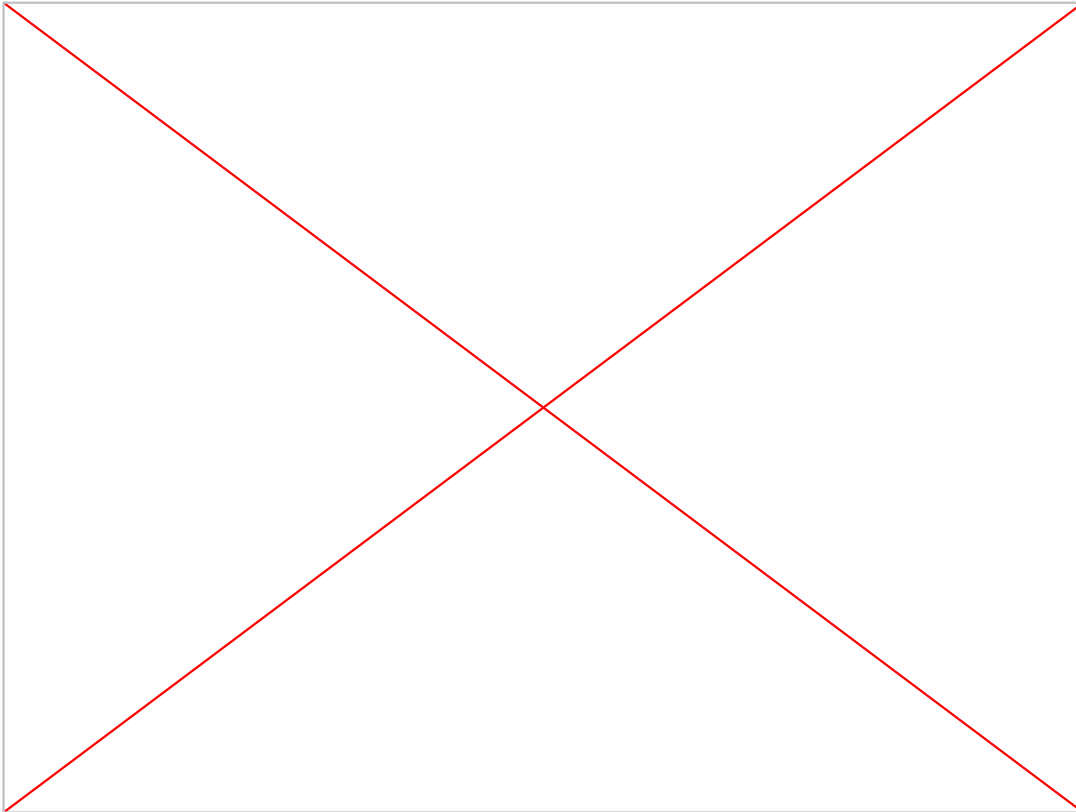
Light-Sheet is faster



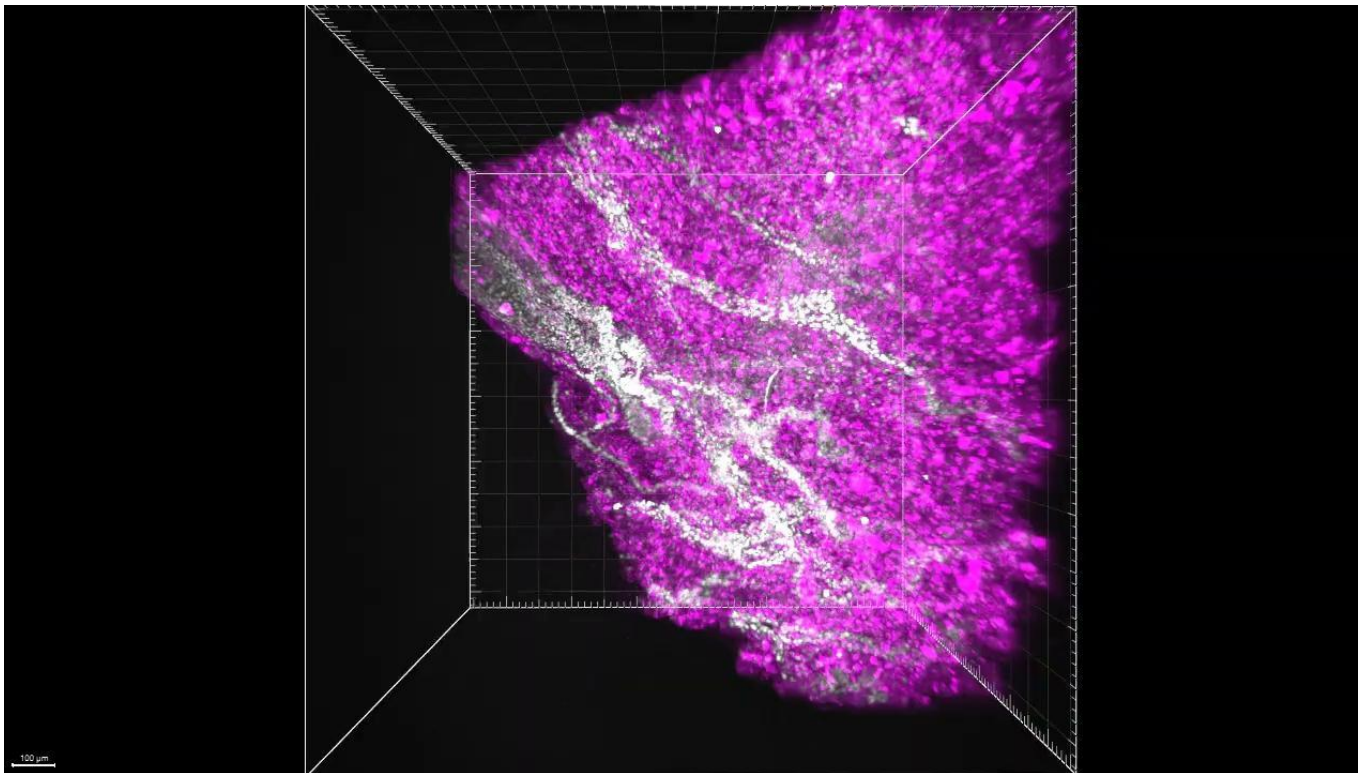
Tissue clearing allows deeper imaging



Light-sheet imaging of colorectal tissue



Visualizing vasculature of healthy colon



Acknowledgements

Leadership



Experiment Design and Techniques



MicRoN



Laboratory Operations



Collaborating physicians/scientists (BWH)



Sample Coordination

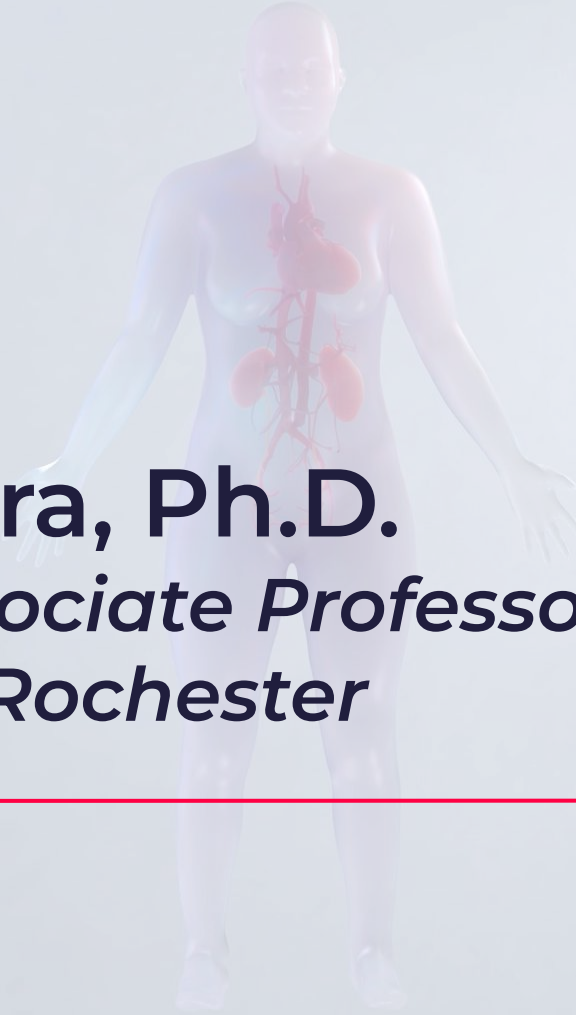


3D Analysis/Imaging (UTSW)



PDOTS





Ravi S. Misra, Ph.D.
Research Associate Professor
University of Rochester

Utilizing multiplex immunofluorescence microscopy to study pediatric lung disease

HuBMAP-Lung TMC

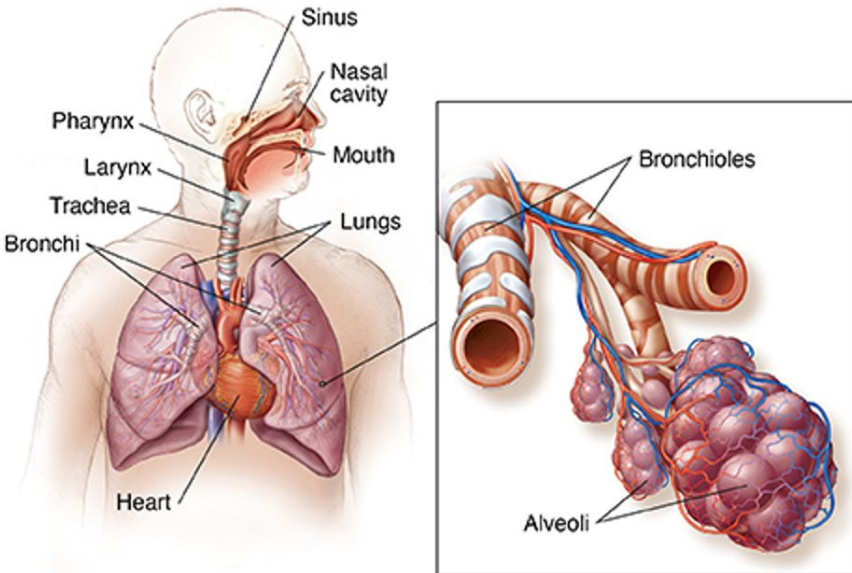
PI /PD(Contact): Gloria Pryhuber

SubAward PIs: Christopher Anderton (OSP), Jeremy Clair (DAC), Gail Deutsch (OSP),
Jim Hagood (OSP), Xin Sun (OSP)

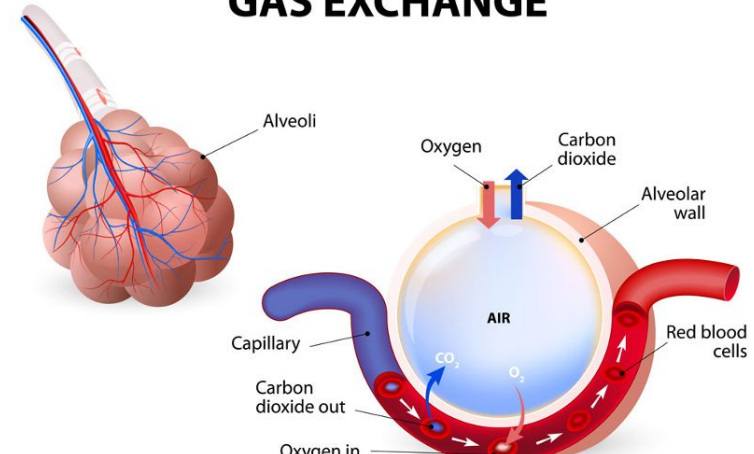
Program Managers: Ravi Misra (OSP), Jeanne Holden-Wiltse (DAC)

Project Manager: Heidie Huyck

An overview of the lung organ and the alveolar gas exchange unit



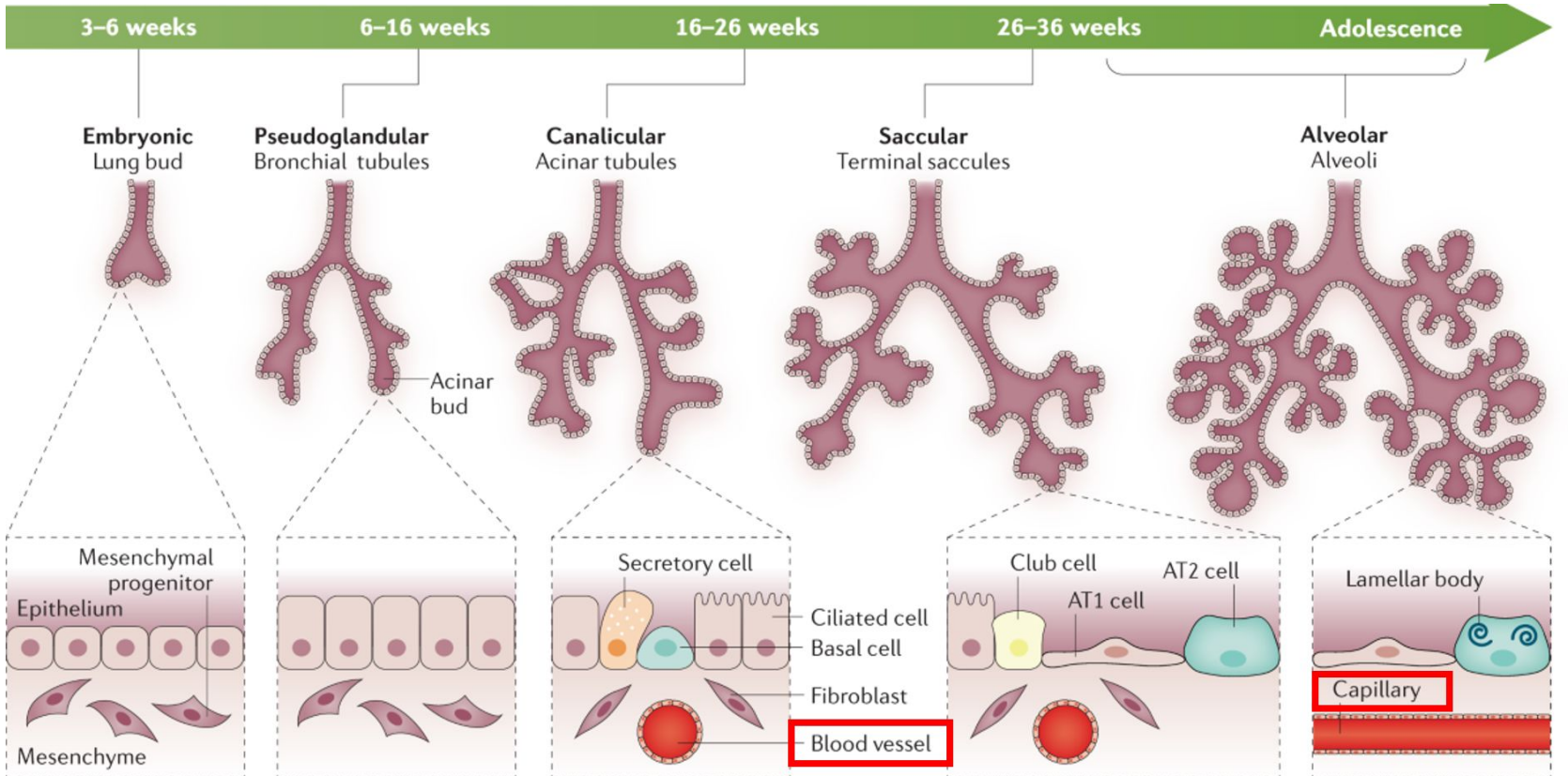
ALVEOLUS GAS EXCHANGE



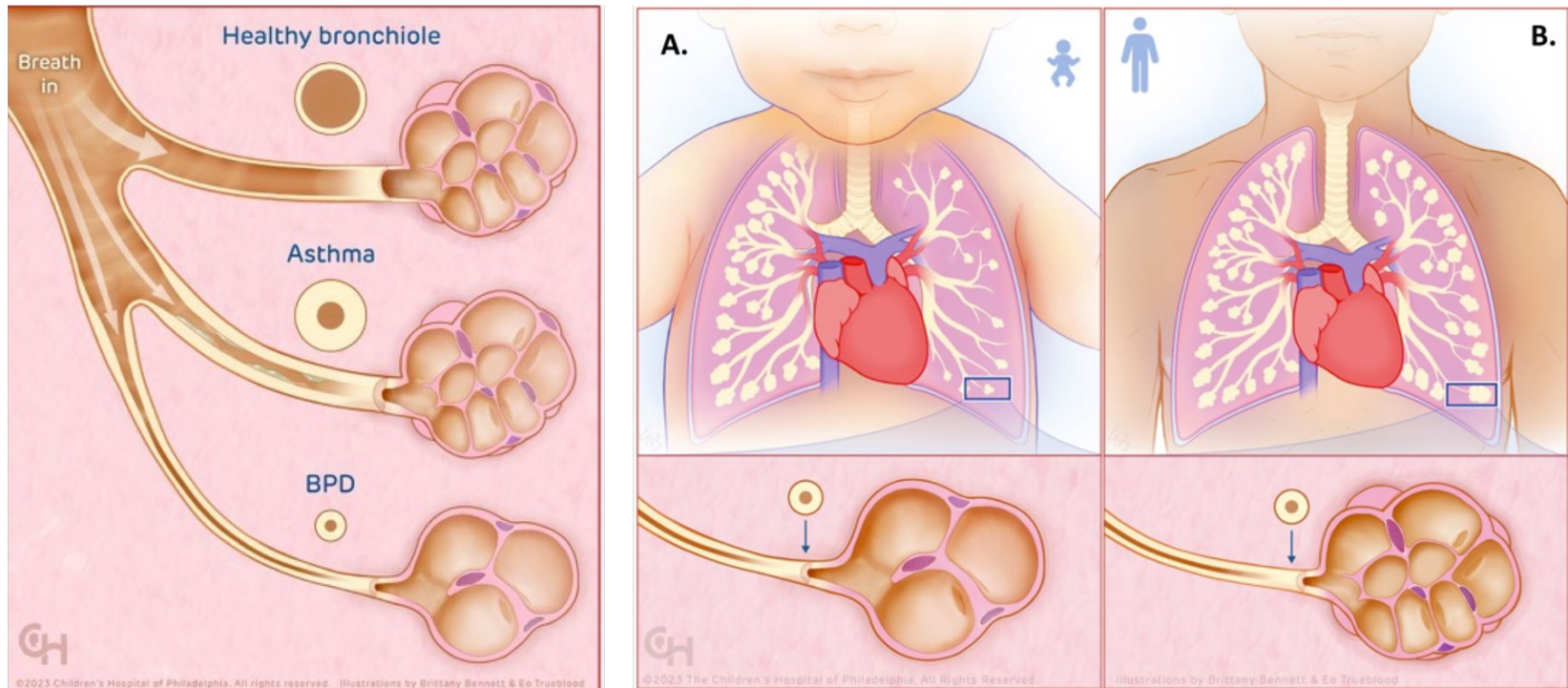
<https://www.spectrumhealthlakeland.org/lakeland-diabetes/diabetes-health-library/Content/85/P01300/>

<https://www.pedilung.com/pediatric-lung-diseases-disorders/anatomy-of-a-childs-lung/alveolus-gas-exchange-pulmonary-alveolus/>

Lung organogenesis: forming a complex organ

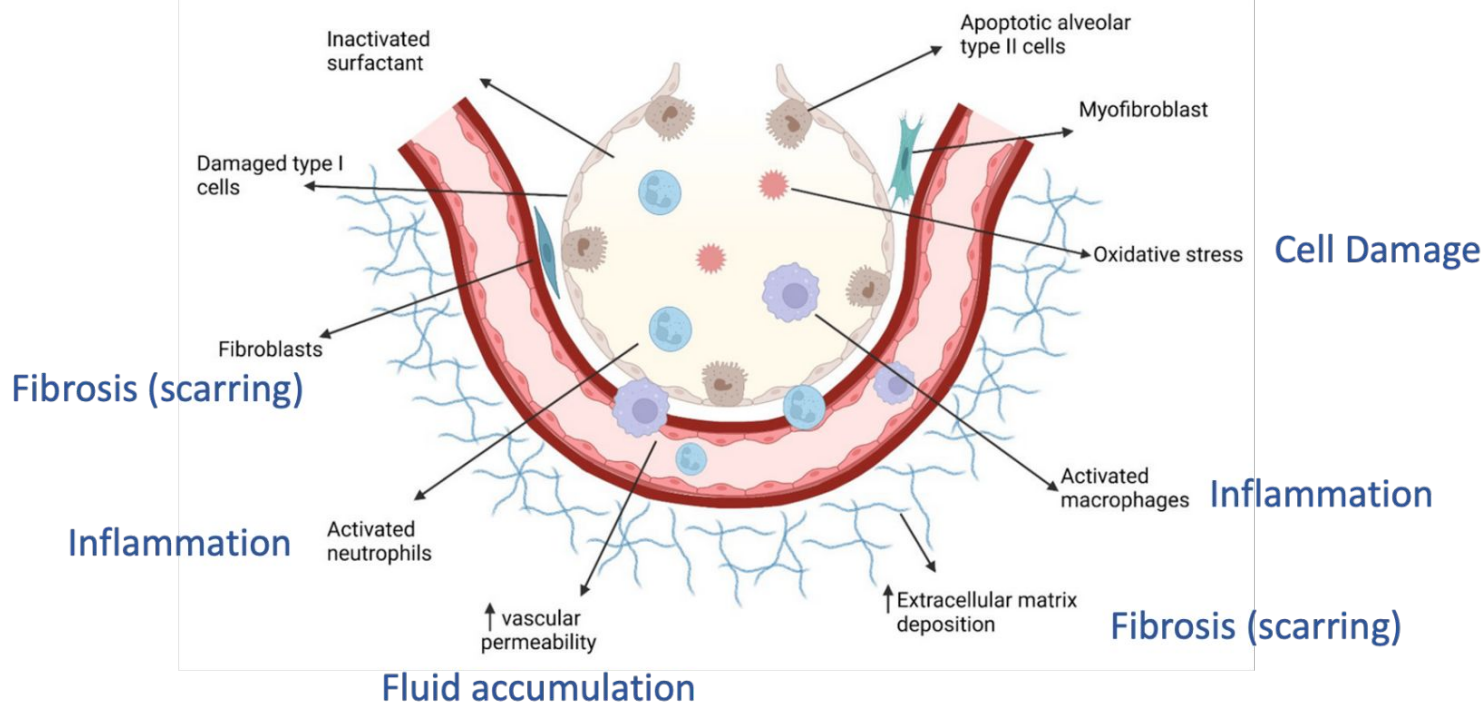


Preterm birth and exposure to hyperoxia can lead to persistent lung damage: Bronchopulmonary Dysplasia

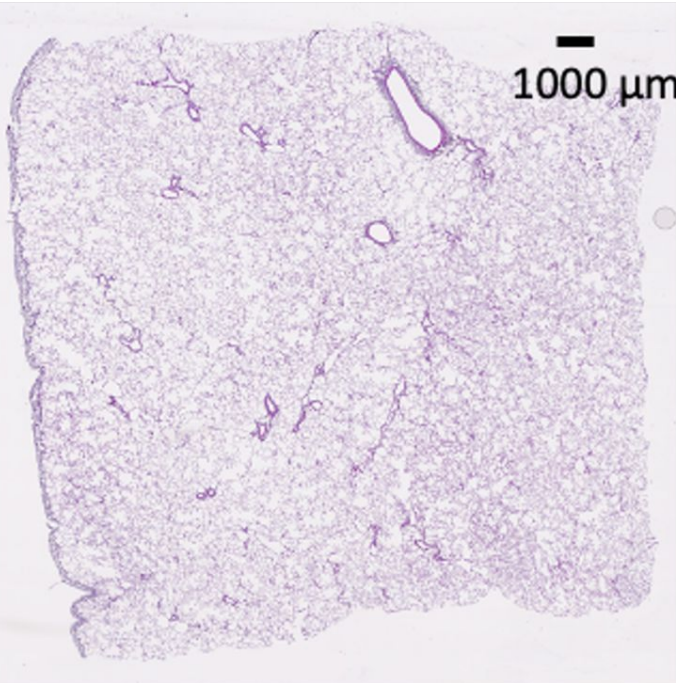


Adapted from <https://www.nature.com/articles/s41372-024-01957-9/>

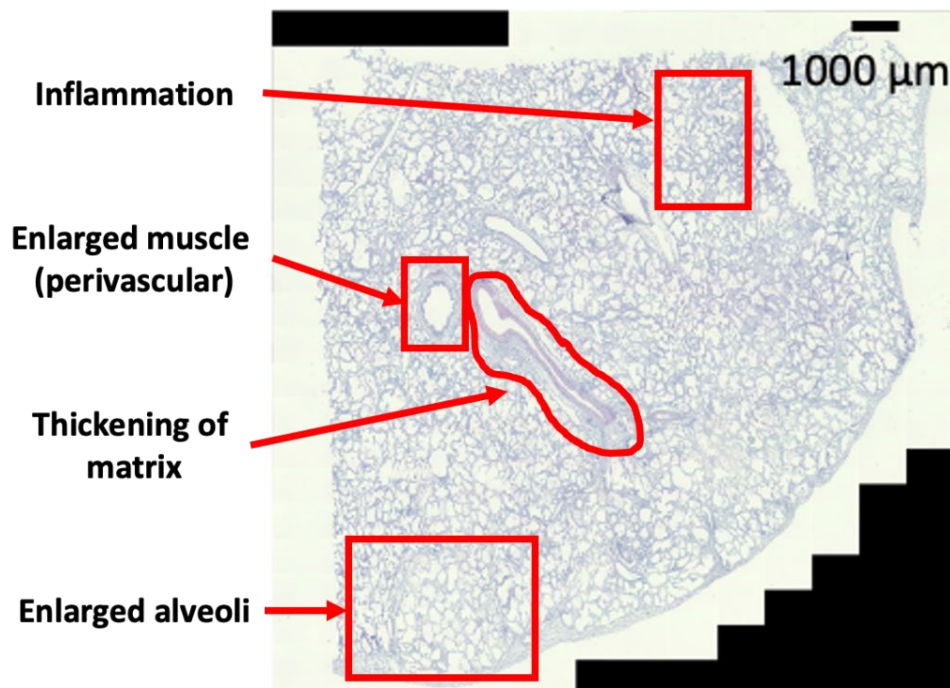
Preterm birth and exposure to hyperoxia can lead to persistent lung damage: Bronchopulmonary Dysplasia



Studying BPD and control lung samples from the BRINDL repository

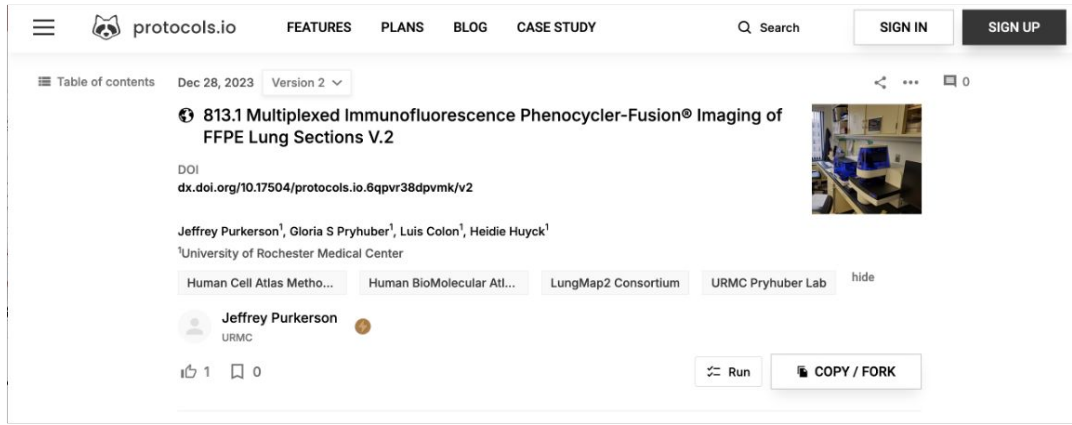


Healthy Lung



BPD Lung

Detecting cell types in the lung using immunofluorescence microscopy (Phenocycler)



The screenshot shows a detailed view of a scientific protocol page. At the top, there's a navigation bar with 'protocols.io' logo, 'FEATURES', 'PLANS', 'BLOG', 'CASE STUDY', a search bar, and 'SIGN IN/SIGN UP' buttons. Below the header, the page displays the 'Table of contents' and the date 'Dec 28, 2023'. A dropdown menu shows 'Version 2'. The main content area features a title '813.1 Multiplexed Immunofluorescence Phenocycler-Fusion® Imaging of FFPE Lung Sections V.2' with a DOI link: 'dx.doi.org/10.17504/protocols.io.6qpvr38dpvmk/v2'. Below the title, authors are listed: Jeffrey Purkerson¹, Gloria S Pryhuber¹, Luis Colon¹, Heidie Huyck¹. The superscript '1' indicates they are from the University of Rochester Medical Center. There are also links to 'Human Cell Atlas Metho...', 'Human BioMolecular Atl...', 'LungMap2 Consortium', and 'URMC Pryhuber Lab'. A small thumbnail image shows a laboratory setup with a Phenocycler instrument. At the bottom of the page, there are social sharing icons ('Run', 'COPY / FORK') and a user profile for 'Jeffrey Purkerson'.

Endothelial Cells

Muscle Cells

Immune Cells

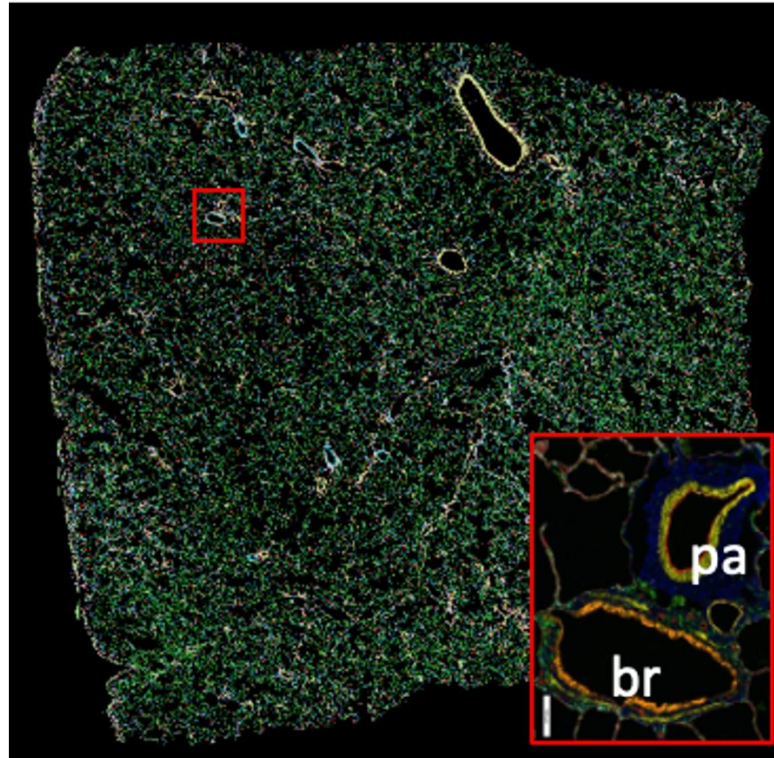
Epithelial Cells

Extracellular Matrix

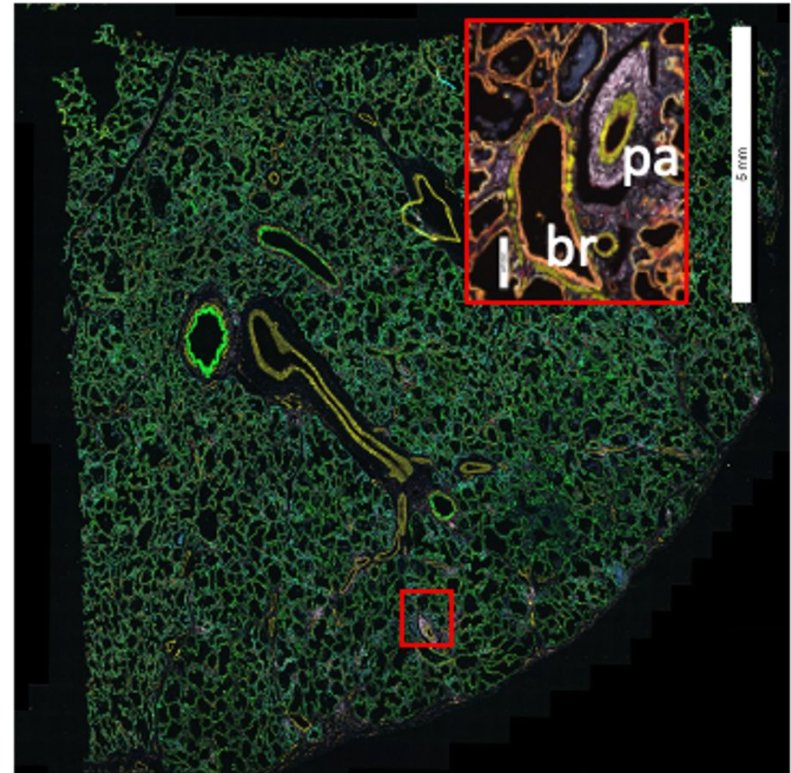
Dr. Jeffery Purkerson

<https://www.protocols.io/view/813-1-multiplexed-immunofluorescence-phenocycler-f-6qpvr38dpvmk/v2>

Imaging of healthy and diseased lung

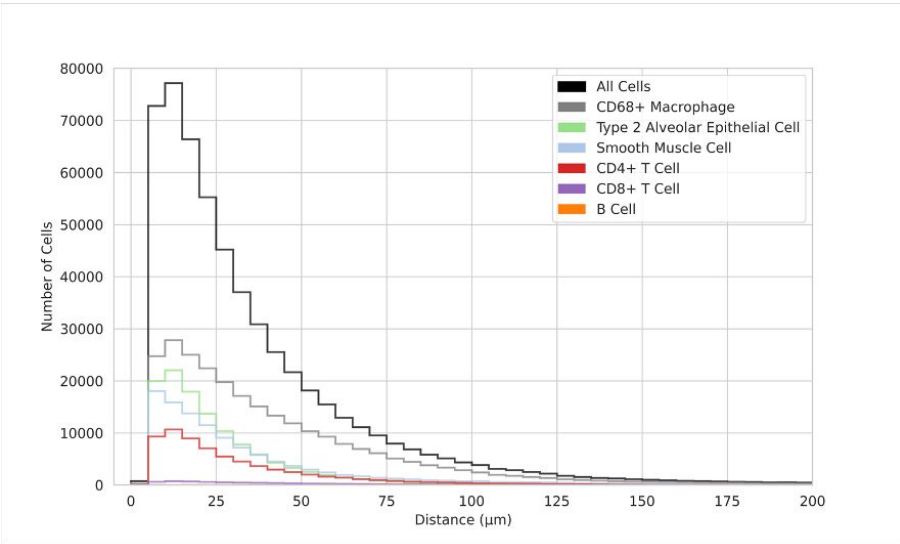


Healthy Lung

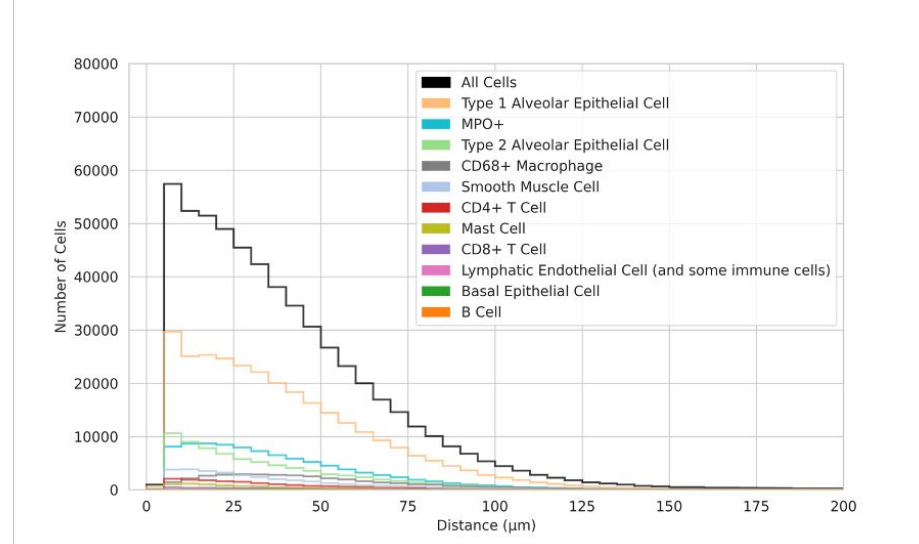


BPD Lung

BPD lungs have a higher number of immune cells near vascular cells



Healthy Lung



BPD Lung

Future work to increase the number of cases and analytes

Reveals beauty and complexity of lung architecture.

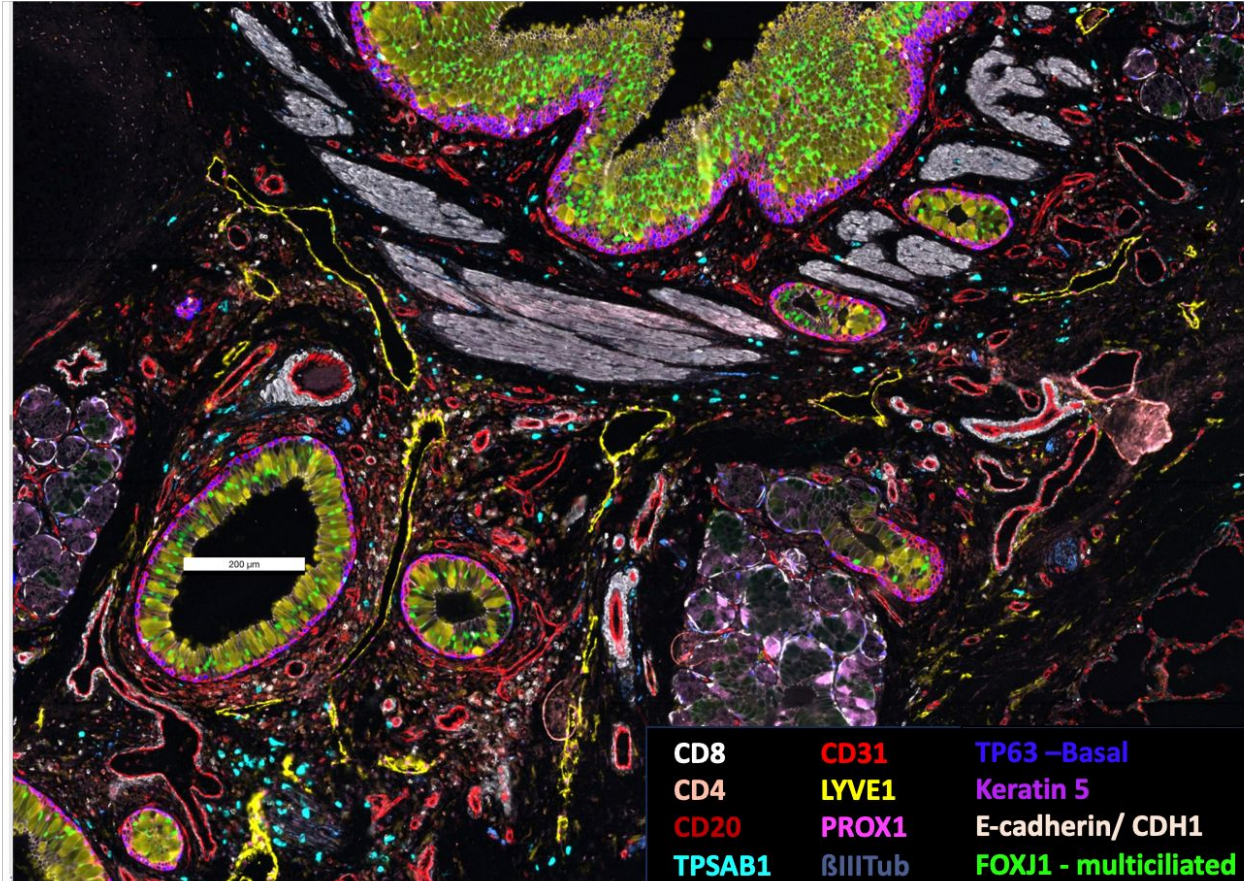
Highly vascular and immune cell rich region around bronchus

Note:

lymphatics,
muscular bronchial blood vessels of varying diameter,
ciliated duct cells,
mast cells,
nerve,

B cell and T cell rich aggregates

5 yo W M, 30 antibody panel



URMC
Tissue, CODEX, Informatics

Gloria Pryhuber, MD
(Contact PI)



Ravi Misra, PhD
Program Manager



Heidie Huyck, BS
Lab & BRINDL Manager



HuBMAP-Lung TMC Village

NIH OPTN NDRI IIAM

LungMAP, HuBMAP, HCA Consortia

PNNL
MPLEX, MSI N-Glycan

Jeremy Clair, PhD Chris Anderton, PhD Jennifer Kyle



U Wash Pathology
Histopathology, QA, Interpretation
Gail Deutsch, MD

Gautam
Bandyopadhyay, PhD



Jeff Purkerson, PhD



Matthew Jehrio, MS



UCSD
Epigenomics, Spatial and sn/scTranscriptomics,
Label Free Imaging

Xin Sun, PhD



Elizabeth Duong, MD



Jamie Verheyden, PhD



Dusan Velickovic, PhD
Brittney Gorman



Josh Adkins, PhD



Anthony Corbett, MS
Lead Res Data Engineer



Jen Dutra, MS



Jeanne Holden-Wiltse,
MPH, MBA



Marti Preston
URMC Grants Manager



Kyle Gaulton, PhD



Rongbo Li



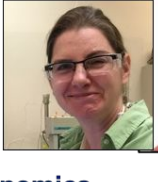
Jisun Chin



Heather Olson



Rosey Chu



URMC

Genomics Res Center
Cameron Baker, MS

John Ashton, PhD



Jeff Malik, PhD



Jeff Malik, PhD



UNC

Small Airway Dissection, GeoMx
Jim Hagood, MD Kenichi Okuda, MD-PhD



SRS Imaging
Lingyan Shi, PhD



UCSD Center for Epigenomics

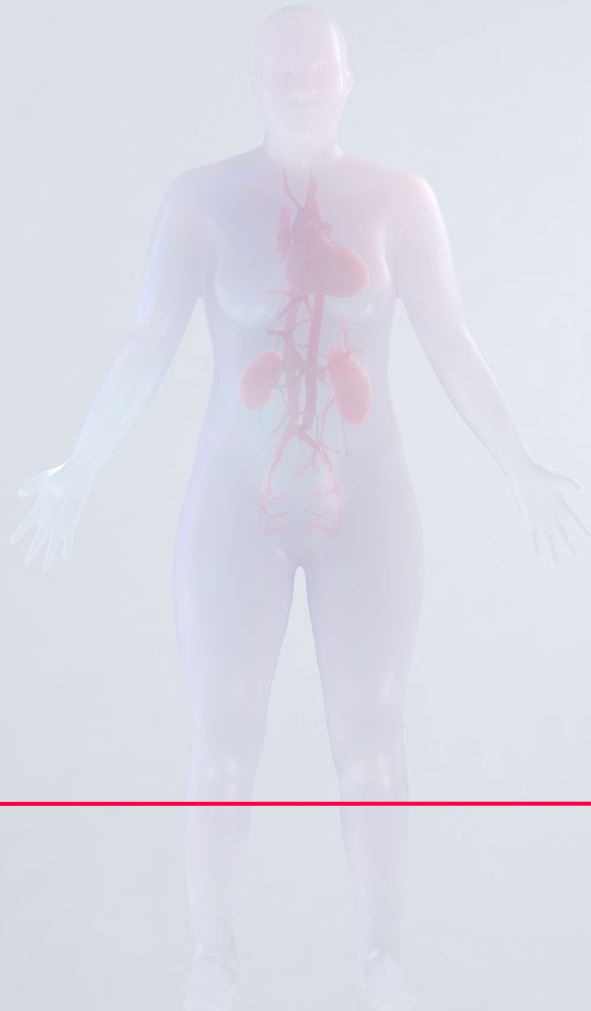
Allen Wang, PhD Quan Zhu, PhD



Kun Zhang, PhD



Q&A



<https://humanatlas.io/events/2024-24h>

Questions

How do we best capture data for a Multiscale Human?

How do we map a Multiscale Human?

How do we model a Multiscale Human?

How can LLMs or RAGs be used to advance science and clinical practice?

Thank you
